


Quantum Coding Transitions in the Presence of Boundary Dissipation

Izabella Lovas^{1,*}, Utkarsh Agrawal,¹ and Sagar Vijay²

¹*Kavli Institute for Theoretical Physics, University of California, Santa Barbara, California 93106, USA*

²*Department of Physics, University of California, Santa Barbara, California 93106, USA*

 (Received 18 August 2023; accepted 3 June 2024; published 7 August 2024)

We investigate phase transitions in the encoding of quantum information in a quantum many-body system due to the competing effects of unitary scrambling and boundary dissipation. Specifically, we study the fate of quantum information in a one-dimensional qudit chain, subject to local unitary quantum circuit evolution in the presence of depolarizing noise at the boundary. If the qudit chain initially contains a finite amount of locally accessible quantum information, unitary evolution in the presence of boundary dissipation allows this information to remain partially protected when the dissipation is sufficiently weak, and up to timescales growing linearly in the system size L . In contrast, for strong enough dissipation, this information is completely lost to the dissipative environment. We analytically investigate this “quantum coding transition” by considering dynamics involving Haar-random, local unitary gates, and confirm our predictions in numerical simulations of Clifford quantum circuits. Scrambling the quantum information in the qudit chain with a unitary circuit of depth $\mathcal{O}(\log L)$ before the onset of dissipation can perfectly protect the information until late times. The nature of the coding transition changes when the dynamics extend for times much longer than L . We further show that at weak dissipation, it is possible to code at a finite rate, i.e., a fraction of the many-body Hilbert space of the qudit chain can be used to encode quantum information.

DOI: [10.1103/PRXQuantum.5.030327](https://doi.org/10.1103/PRXQuantum.5.030327)

I. INTRODUCTION

The chaotic unitary evolution of an isolated quantum system will spread initially localized quantum information over nonlocal degrees of freedom, a process known as quantum information scrambling [1–4]. This delocalization of information aids in protecting quantum information against local noise, which is present in any real physical system. Studying the robustness of quantum information in the presence of both unitary scrambling and dissipation is important both to understand new dynamical regimes of quantum many-body dynamics, and from a practical standpoint, to design quantum codes and to appropriately interpret studies of quantum many-body evolution in near-term quantum simulators. While dissipative dynamical phases of matter have been the subject of intense research for decades [5–9], understanding the dynamics of quantum information in this context opens a new perspective.

Understanding the spreading of information in unitary evolution has led to a deeper understanding of quantum chaos and thermalization [2,10–16], suggesting that investigating the dynamics of quantum information in dissipative systems can shed light on the structure of (possibly new) dynamical regimes of quantum matter.

Besides its fundamental relevance for the dissipative dynamics of generic quantum systems, the fate of quantum information in the presence of unitary scrambling and destructive local noise or measurements has been explored in the context of quantum information theory, leading to the development of the theory of quantum error-correcting codes [17–20]. A key result in the theory of quantum error correction (QEC) is the threshold theorem, stating that, for error rates below some threshold, one can reverse the effects of the errors by applying additional quantum gates [21–23]. In other words, it is possible to correct errors faster than they are created.

The threshold theorem is essential in designing fault-tolerant quantum computers. Applying additional gates, trying to preserve the code space against the noise, allows one to perform logical operations for long times with high precision. Such an active error correction is feasible in artificial quantum systems with a “digital” architecture, in which real-time measurements and unitary evolution can be executed over targeted degrees of freedom. However,

*Corresponding author: izabellalovas@ucsb.edu

Published by the American Physical Society under the terms of the [Creative Commons Attribution 4.0 International](https://creativecommons.org/licenses/by/4.0/) license. Further distribution of this work must maintain attribution to the author(s) and the published article’s title, journal citation, and DOI.

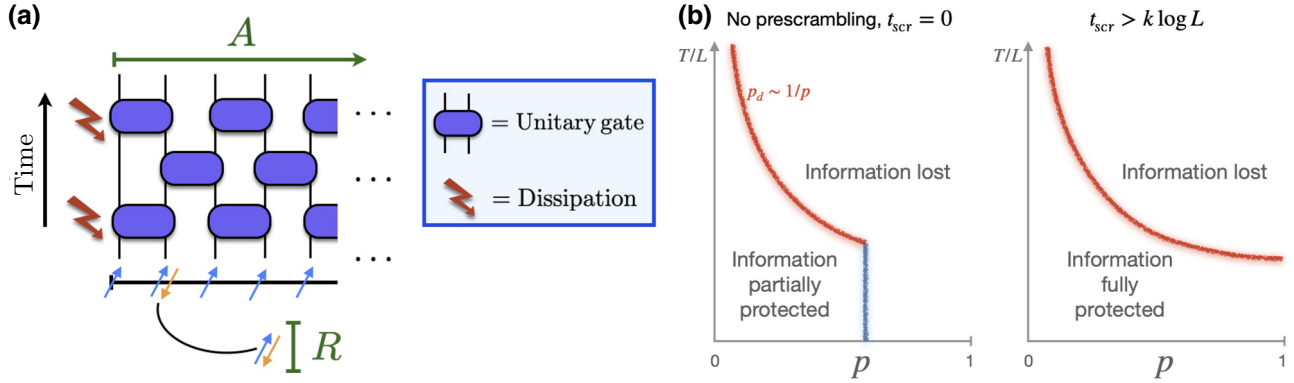


FIG. 1. (a) Quantum information is encoded in a qudit chain through entangling with a reference qudit R . The qudit chain subsequently evolves with a “brickwork” array of Haar-random, two-site unitary gates and dissipation at the boundary. One time step of these dynamics corresponds to two layers of unitary gates along with depolarizing noise at the boundary, as shown schematically in (a). Phase diagrams hosting coding transitions are shown in (b), for localized encoding near the boundary (left), and in the presence of a unitary prescrambling step delocalizing the information before the onset of dissipative dynamics (right). Left: the blue critical line indicates a continuous coding transition with a total number of time steps $T \lesssim L/p$, only occurring for localized encoding in the vicinity of the boundary (see Sec. III). In a statistical mechanical description of the dynamics of quantum information, this transition corresponds to the depinning transition of an Ising domain wall (see Sec. II). The red critical line is a first-order coding transition with $T \gtrsim L/p$. Across this line, as the system approaches thermalization, it becomes maximally entangled with the environment, resulting in information loss (see Sec. IV). Right: performing unitary prescrambling on timescales scaling logarithmically with the system size increases the robustness of encoding and can perfectly protect the information up to timescales $T \sim L/p$.

in analog quantum simulators realized, e.g., with ultracold atoms, the options for active error correction are more restricted and costly due to the limited control over the dynamics. This provides a strong motivation for exploring whether the system’s intrinsic dynamics alone can protect information, by hiding it from destructive local noise. Despite this fundamental relevance, the conditions for obtaining such a robust, self-generated coding dynamics in a generic quantum system without any degree of external control, are still not fully explored.

Recently, the robustness of a self-generated code space against a special class of local perturbations has been investigated, taking the form of local projective measurements. These studies revealed a phase transition driven by the measurement rate, such that the code space can store an extensive amount of information, as long as the rate of measurements remains below a finite threshold [24–28]. However, this result cannot be generalized to more generic noise channels. For example, a quantum many-body system evolving in the presence of random erasures occurring in the bulk with a finite rate destroys all quantum information in constant time [29,30], and active error correction during the dynamics is required to protect the information beyond this timescale. Understanding the conditions (if any) that unitary evolution and local errors have to satisfy to guarantee the emergence of a robust, self-generated code space, without the need for an active error correction during the dynamics, is an open question of utmost relevance.

A. Summary of results

With these motivations, we take a step towards understanding the dynamics of quantum information under generic scrambling and local noise, by exploring the fate of quantum information, subjected to the competing effects of boundary dissipation and unitary spreading in a one-dimensional chaotic quantum system. For concreteness and simplicity, we focus on the setup sketched in Fig. 1(a), showing the first few layers of a random quantum circuit with a depolarization channel acting at the left boundary. We note that it is known in both classical coding theory [31–35] and the quantum case [36–38] that random unitary dynamics provides an optimal encoding of information. We entangle one external reference qudit R near the boundary into a maximally entangled pair, thereby encoding one qudit of quantum information initially localized near the dissipative boundary. Our results summarized below do not depend on the precise distance between this entangled pair and the dissipative boundary, as long as it remains finite in the thermodynamic limit. For concreteness, in all of the numerical simulations presented in this paper, we choose to entangle the leftmost qudit, such that the quantum information is encoded right at the dissipative boundary. We then ask what happens to this information as the system is subject to noisy dynamics, up to timescales T scaling linearly with the system size L , such that T/L is fixed. We note that we are focusing on random circuits without any symmetries, consisting of “generic” unitary gates, i.e., gates that increase the

entanglement between subsystems linearly in time until saturation. Under these conditions, the reduced density matrix of subsystems approaches a maximally mixed density matrix at late times, a process that can be interpreted as thermalization towards infinite effective temperature. We use the term “thermalization” in this sense throughout the paper. Importantly, by taking the thermodynamic limit $L \rightarrow \infty$ and the long time limit $T \rightarrow \infty$ simultaneously, with T/L constant, we probe the system on timescales where it is expected to thermalize [12].

Interestingly, we find that this quantum information can remain robust even at these long times, giving rise to a rich dynamical phase diagram as a function of dissipation strength p and the ratio T/L . Our main results, supported both by analytical arguments for general qudit systems, and numerical simulations performed on qubit chains, are summarized in Fig. 1(b). The left panel shows the case where the noisy dynamics starts immediately after the encoding of the quantum information locally, near the leftmost boundary. We find a dissipation-induced quantum coding phase transition, separating a region where the coherent information remains partially protected and gets delocalized within the system, and a phase where all of this information leaked to the environment. The nature of the coding transition, however, depends on the ratio T/L . For $T/L \lesssim 1$, the right boundary is effectively decoupled from the dynamics of information and we observe a continuous second-order phase transition (blue line). For even larger ratios T/L , the right boundary plays a crucial role and gives rise to a first-order phase transition (red). We also demonstrate that adding a unitary “prescrambling” step after the local encoding, before the onset of the dissipative dynamics, can efficiently increase the robustness of the encoded information. In particular, as shown in the right panel of Fig. 1(b), a prescrambling time t_{scr} scaling logarithmically with the system size, $t_{\text{scr}} \sim \log L$, ensures that quantum information remains perfectly protected for small enough dissipation strengths p , up to timescales $T \sim L/p$.

We gain a detailed understanding of these different types of coding transitions, by mapping the dynamics of quantum information in a qudit chain, governed by a circuit with Haar-random unitary gates and boundary dissipation, to the statistical mechanics of a two-dimensional lattice magnet. This mapping, which has been extensively employed to understand unitary circuit quantum dynamics as well as dynamics with projective measurements (see Refs. [39,40] for a review), allows us to obtain analytical predictions, as well as instructive numerical results. While the entanglement measures of interest that diagnose the quantum coding transition require taking a formal replica limit of this lattice magnet (akin to a limit arising when considering “quenched” disorder), we focus our attention on understanding this lattice magnet away from the replica limit (akin to studying an “annealed” disorder average). Specifically, we focus on the “annealed” disorder average

of the second Rényi mutual information between the output of the circuit, A , and the reference qubit R . In this limit, the circuit with the boundary depolarization can be mapped to the statistical mechanics of an Ising magnet, in which a single Ising domain wall experiences an attractive or repulsive potential at one boundary of the two-dimensional system, whose strength is tuned by the dissipation strength. In this language, the coding transition at times $T/L \lesssim 1$ can be understood as a second-order pinning-depinning transition of the Ising domain wall at the noisy boundary; we provide conjectures as to the true nature of this transition in the replica limit. At later times $T/L > 1/p$, the right boundary gives rise to a different, first-order transition by “absorbing” the Ising domain wall. Insights gained from this classical statistical picture, valid for general qudit chains, are confirmed by large-scale numerical simulations performed on qubit systems evolving according to Clifford quantum random circuits.

Finally, we show that the coding transition for $T/L > 1/p$ can also be understood as a transition arising from the monogamy of entanglement. At such late times, as the system of L qudits becomes entangled with a growing number of environmental degrees of freedom, scaling as pT , eventually it can no longer stay simultaneously entangled with the reference qudit, and all information leaks to the environment. We conclude with the interesting scenario of encoding an extensive amount of information in the system. Specifically, we show that a similar coding transition persists when we entangle an extensive number of reference qudits into maximally entangled pairs with the qudits of the system. In particular, we identify two threshold values for the dissipation strength p , $p_{\text{th},1}$ and $p_{\text{th},2}$, separating three regions according to the behavior of the information density. The information density is perfectly protected in the system for $p < p_{\text{th},1}$, while it starts to leak into the environment above this threshold. A finite density of information still survives in the region $p_{\text{th},1} < p < p_{\text{th},2}$, until eventually reaching zero at the upper threshold $p_{\text{th},2}$. As before, we supplement our analytical results for qudit chains with numerical simulations performed on qubit systems.

The rest of the paper is organized as follows. In Sec. II, we lay the foundations for our analytical considerations of the quantum coding phase transitions in general qudit chains. To this end, we introduce the mapping between the coherent quantum information in random circuits and the properties of an Ising domain wall experiencing a repulsive or attractive boundary on the left and an absorbing boundary on the right, by considering the “annealed” second Rényi mutual information between the circuit output and the encoded information. We derive the random walk model in Sec. II A. We then show in Sec. II B that different phases on either side of the coding transition can be understood by inspecting the weighted trajectories of the Ising domain wall in this statistical mechanical model.

We turn to the detailed discussion of the second-order coding transition in the regime $T \lesssim L/p$, induced by the dissipative boundary alone without the interference of the clean boundary, in Sec. III. We first rely on the random walk model to gain a qualitative understanding of the phase transition in qudit systems, and discuss the classical pinning-depinning transition of the Ising domain wall in Sec. III A. Building on these insights, we turn to qubit systems and verify the presence of the quantum coding transition and study its properties numerically in Sec. III B, by performing large-scale numerical simulations on Clifford quantum circuits. We return to our analytical arguments and discuss the nature of this transition in more detail in Sec. III C. To end the section, in Sec. III D we comment on increasing the robustness of the encoded information by applying a unitary prescrambling before the onset of dissipative dynamics. Through a combination of analytical calculations in qudit systems and numerical simulations on qubit chains we show that a prescrambling time t_{scr} scaling logarithmically with the system size provides perfect protection for the coherent information for weak enough dissipation p , up to timescales $T/L \sim O(1)$.

We turn to the first-order coding transition, induced by the interplay of the dissipative left boundary and the clean right boundary at times $T \gtrsim L/p$, in Sec. IV. First, we discuss how this phase transition can be understood in the statistical mechanical framework as the absorption of the entanglement domain wall by the right boundary and is driven by the monogamy of entanglement as the system becomes entangled with a growing number of environmental qudits. We present and analyze the numerical results obtained from Clifford circuit simulations on qubit chains in Sec. IV A, and find good agreement with the predictions of the statistical mechanics of the Ising lattice magnet. We argue that this coding transition is of first order, and discuss its scaling properties in Sec. IV B. Finally, Sec V serves as an outlook to the case of encoding an extensive amount of information into the system. Here we consider entangling a finite density of reference qudits with the system, and find a monogamy-induced coding transition at late times $T \gtrsim L/p$, similar to that observed for a single qudit of quantum information. Here we find three phases, with the information perfectly protected for $p < p_{\text{th},1}$, a finite density of information surviving for $p_{\text{th},1} < p < p_{\text{th},2}$, and the density reaching zero above $p_{\text{th},2}$. We conclude by summarizing our results, and discussing open questions in Sec. VI.

II. DISSIPATION IN QUANTUM CIRCUIT EVOLUTION

A. Statistical mechanics of random unitary evolution and dissipation

Past studies of random local unitary evolution [39,40] and evolution with projective measurements

[24–26] and with dissipation [29,30,41–46] have uncovered a wealth of universal structures governing the dynamics of information-theoretic quantities such as the Rényi entanglement entropy. Averaging over an ensemble of unitary gates in this setting gives rise to an emergent classical statistical mechanics of quantum entanglement, which must be understood in an appropriate “replica limit” in order to recover the behavior of the information-theoretic quantities of interest. A qualitatively accurate understanding of the behavior of quantum entanglement in chaotic unitary dynamics and in dynamics with projective measurements can still be obtained even without taking the replica limit [13,47–49], though these approaches often fail to capture quantitative, universal properties characterizing distinct regimes of quantum many-body evolution (e.g., of the volume-law-entangled phase of infrequently monitored quantum many-body evolution [50]) or of critical points (e.g., separating different phases of monitored quantum dynamics).

Here, we consider the evolution of qudits under random, local unitary gates and boundary dissipation. Averaging over the ensemble of unitary gates, in the calculation of the evolving *purity* of the subsystem, leads to an emergent statistical mechanics of an Ising magnet. We present the various ingredients that the unitary evolution and dissipation correspond to in this setting, before using these ingredients extensively in subsequent sections to understand the stability of encoded quantum information under this evolution.

We focus our attention on a one-dimensional chain of qudits, with Hilbert space dimension q at each lattice site. The dissipation acts on the boundary qudit, and is described by the depolarizing channel Φ acting on the density matrix ρ of this qudit as

$$\Phi(\rho) = (1 - p) \rho + p \cdot \frac{\mathbb{1}_{q \times q}}{q} \quad (1)$$

with $p \in [0, 1]$ parameterizing the “strength” of the dissipation. For future convenience, we choose to rewrite the depolarizing channel as an *operator* $\hat{\Phi}$ that acts within a Hilbert space of dimension q^2 . The operator $\hat{\Phi}$ takes the form

$$\hat{\Phi} = \sum_{i,j=1}^q \left[(1 - p) |i,j\rangle \langle i,j| + \frac{p}{q} |i,i\rangle \langle j,j| \right], \quad (2)$$

where $|i\rangle$ for $i \in \{1, \dots, q\}$ denotes an orthonormal basis of states of a single qudit [51].

Apart from the dissipation, the remaining qudits will be chosen to evolve according to two-site unitary gates, chosen from the uniform (Haar) measure for the unitary group $U(q^2)$. Given such a two-qudit unitary gate U , we note that the average over the Haar measure of $U \otimes U^* \otimes U \otimes$

U^* —a quantity that will naturally appear in subsequent sections—is given by

$$\begin{aligned} V &\equiv \langle U \otimes U^* \otimes U \otimes U^* \rangle \\ &= \sum_{\sigma, \tau \in \{\uparrow, \downarrow\}} \text{wg}_2(\sigma\tau) |\tau, \tau\rangle \langle \sigma, \sigma|, \end{aligned} \quad (3)$$

where $\langle \cdot \rangle$ denotes the Haar average, the Weingarten function is given as $\text{wg}_2(+) = q^2/(q^4 - 1)$ and $\text{wg}_2(-) = -1/(q^4 - 1)$, and states $|\uparrow\rangle$ and $|\downarrow\rangle$ are defined as $|\uparrow\rangle \equiv \sum_{i,j=1}^q |i, i, j, j\rangle$ and $|\downarrow\rangle \equiv \sum_{i,j=1}^q |i, j, j, i\rangle$ so that

$$\langle \sigma | \tau \rangle = (q^2 - q)\delta_{\sigma, \tau} + q. \quad (4)$$

From these expressions, it is clear that

$$V|\uparrow\uparrow\rangle = |\uparrow\uparrow\rangle, \quad V|\downarrow\downarrow\rangle = |\downarrow\downarrow\rangle, \quad (5)$$

$$V|\uparrow\downarrow\rangle = V|\downarrow\uparrow\rangle = \frac{q}{q^2 + 1} [|\downarrow\downarrow\rangle + |\uparrow\uparrow\rangle]. \quad (6)$$

From Eq. (2), the operator $D \equiv \hat{\Phi} \otimes \hat{\Phi}$ acts on these states as

$$D|\uparrow\rangle = |\uparrow\rangle, \quad D|\downarrow\rangle = (1 - p)^2 |\downarrow\rangle + \frac{p(2 - p)}{q} |\uparrow\rangle. \quad (7)$$

B. Boundary dissipation and the encoding of quantum information

We now consider a qudit chain consisting of L qudits, into which quantum information has been encoded. We may imagine that this quantum information is represented by physical reference qudits that are maximally entangled with the one-dimensional system. This system subsequently evolves according to a unitary circuit composed of Haar-random unitary gates in a “brickwork” array, together with dissipation that acts near the boundary. We note that the Haar-random quantum circuit governing the unitary part of the evolution allows the efficient scrambling of information, providing a convenient setting to study the dynamics of generic chaotic quantum many-body systems [39]. We first focus on the case where only a single qudit is encoded in the one-dimensional system, and with dissipation acting periodically in time on the boundary qudit, as shown schematically in Fig. 2(a). A single time step of this evolution corresponds to the application of two layers of two-site unitary gates, followed by the depolarizing channel (1) on the boundary qudit.

To diagnose whether this qudit of encoded information can remain in the system, even as the boundary dissipation continues to act, we study the behavior of the bipartite mutual information between the reference qudit (R) and the

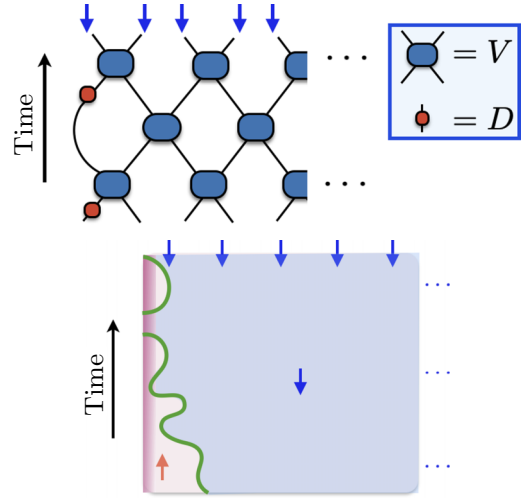


FIG. 2. Top: Haar-averaged purity of the evolving state mapped to an Ising magnet. The time-evolved purity involves two forward and two backward copies of the random circuit. Performing a Haar average over the unitary gates gives rise to an Ising partition function, expressed as the product of transfer matrices defined in Eqs. (5)–(7). Matrix V emerges from the average over two forward and two backward replicas of unitary gates U , and D represents dissipation at the boundary. Bottom: a coarse-grained description of this Ising magnet involves a single Ising domain wall (green) in the presence of a boundary magnetic field (shaded red). The boundary conditions at the bottom of the Ising magnet, which are fixed by the initial state of the quantum system, are not shown.

system (A) at time t ; this mutual information is defined as

$$I_{A,R}(t) = S_A(t) + S_R(t) - S_{A \cup R}(t), \quad (8)$$

where $S_A \equiv -\text{Tr}[\rho_A(t) \log_q \rho_A(t)]$ is the von Neumann entanglement entropy of subsystem A at time t . We note that $I_{A,R}(t)$ is related to the coherent information present in the system. If $I_{A,R} = 2$, the entangled qudit can be perfectly recovered by applying a recovery operation to the system *alone*, whereas, for $I_{A,R} = 0$, the information has leaked to the environment, that is, $I_{E,R} = 2$ [52]. Importantly, when $I_{A,R} = 2 - \epsilon$ for some small $\epsilon > 0$, the entangled qudit can be recovered with fidelity $F > 1 - 2\sqrt{\epsilon}$ [53].

The mutual information (8) averaged over realizations of the random unitary evolution thus diagnoses whether quantum information remains in the system, even in the presence of boundary dissipation. Instead of considering the Haar average of the mutual information, we turn our attention on the “annealed” average of the second Rényi mutual information between A and R , defined as

$$I_{A,R}^{(\text{ann})}(t) \equiv \log_q \langle q^{I_{A,R}^{(2)}(t)} \rangle, \quad (9)$$

where $I_{A,R}^{(2)}(t) = S_A^{(2)}(t) + S_R^{(2)}(t) - S_{A \cup R}^{(2)}(t)$, with the second Rényi entropy defined as $S_A^{(2)} \equiv -\log_q \text{Tr} \rho_A(t)^2$, and $\langle \cdot \rangle$

denotes the Haar average over the unitary gates in the circuit. The behavior of the annealed mutual information (9) is also expected to capture the qualitative behavior of quantum information recovery since $I_{A,R}^{(\text{ann})} = 2$ if and only if $I_{A,R} = 2$. Though the quantitative details of the annealed information may differ from the true mutual information, as we later clarify. We also note that a similar quantity called “mutual purity” $\mathcal{F}(A : R) = \text{Tr}\rho_{A,R}^2 - \text{Tr}\rho_A^2\text{Tr}\rho_R^2$ was recently studied in Ref. [54]. It was shown that mutual purity also provides a diagnostic for the possibility of recovery of quantum information.

We proceed to calculate the annealed mutual information (9). We initialize the qudits in a product state, except for the qudit at a site x_0 away from the boundary that is maximally entangled with the reference qudit. As the system evolves in the presence of unitary gates and dissipation, it is evident that the purity of the reference qudit remains unchanged, $\text{Tr}\rho_R(t)^2 = q^{-1}$ for all times t . Furthermore, calculation of $\langle \text{Tr}\rho_A(t)^2 \rangle$ and $\langle \text{Tr}\rho_{AUR}(t)^2 \rangle$ involves performing a Haar average of four copies of the quantum circuit. Following the discussion in the previous section, it is thus clear that these Haar-averaged purities may be written as partition functions for an Ising magnet of finite extent in the vertical direction—corresponding to the time direction in the quantum circuit—and with horizontal extent fixed by the number of qudits in the system. The Ising spins live on the links of a square lattice, and are acted upon by the transfer matrices V and D , as given in Eqs. (5), (6), and (7), depending on whether a Haar-random unitary gate or dissipation is applied at a particular point in spacetime in the quantum circuit, respectively. The full transfer matrix is shown schematically in Fig. 2(b).

The boundary conditions for the Ising partition sum at the bottom and top boundaries are respectively determined by the initial state of the qudit chain along with the location of the reference qudit, and the subsystem over which the purity is being calculated. First, fixing Ising spins at the top boundary to be in the \downarrow state corresponds to keeping the corresponding qudit within the region for which the purity is being calculated. As a result, the spins at the top boundary are all fixed in the \downarrow state for the calculation of both $\langle \text{Tr}\rho_A(t)^2 \rangle$ and $\langle \text{Tr}\rho_{AUR}(t)^2 \rangle$, as shown in Fig. 2(b). These two purities thus only differ in their bottom boundary conditions. Here, the boundary spins are allowed to freely fluctuate, with the exception of the spin corresponding to the qudit at a distance x away from the boundary; the state of this Ising spin determines whether the reference qudit is included in the subsystem whose purity is being computed. More precisely, this spin is fixed in the \uparrow or \downarrow state in the calculation of $\langle \text{Tr}\rho_A(t)^2 \rangle$ and $\langle \text{Tr}\rho_{AUR}(t)^2 \rangle$, respectively.

It is convenient to evaluate these partition functions by contracting the transfer matrix from the top boundary condition, i.e., “backwards” in time with respect to the arrow of time in the quantum circuit. Let $Z(t)$ denote the

partition sum obtained by evolving the all-down state of the Ising spins for t time steps by repeatedly applying the row transfer matrix corresponding to a single time step of the dynamics. The partition sum $Z(t)$ describes a single, directed Ising domain wall, which can only be created or annihilated at the boundary of the system. This can be seen as follows. First, starting with the all-down state, dissipation (7) can flip the boundary Ising spin from $|\downarrow\rangle$ to $|\uparrow\rangle$, thus creating an Ising domain wall near the boundary. The effect of the Haar-random unitary gates (5) and (6) in the bulk of the quantum circuit is to simply move the domain wall. Notably, Eq. (5) implies that the Haar-random gates cannot create or annihilate Ising domain walls in the bulk of the system, though gates acting near the boundary can annihilate the Ising domain wall. Once the state of the boundary spin is $|\uparrow\rangle$, the dissipation cannot alter this state since $D|\uparrow\rangle = |\uparrow\rangle$; this is simply a consequence of the fact that the depolarizing channel (1) leaves the maximally mixed density matrix $\rho = \mathbb{1}_{q \times q}/q$ unchanged.

The partition sum $Z(t)$ is thus performed over histories of the entanglement domain wall trajectories, which can propagate in the bulk of the system, or be created or annihilated at the boundary. Formally, we write

$$Z(t) = \sum_{x \geq 0} z(x, t), \quad (10)$$

where $z(x, t)$ is a restricted sum over trajectories of the entanglement domain wall where the domain wall ends up between sites $x - 1$ and x at time t . In this convention, $z(0, t)$ corresponds to trajectories where the entanglement domain wall no longer exists at time t , as it has been annihilated at the left interface.

We may now write the Haar-averaged purities as

$$\langle \text{Tr}\rho_A(t)^2 \rangle = q^2 \sum_{y > x_0} z(y, t) + q \sum_{y \leq x_0} z(y, t), \quad (11)$$

$$\langle \text{Tr}\rho_{AUR}(t)^2 \rangle = q^2 \sum_{y \leq x_0} z(y, t) + q \sum_{y > x_0} z(y, t). \quad (12)$$

This is due to the fact that $\langle \text{Tr}\rho_{AUR}(t)^2 \rangle$ involves a sum over trajectories of the entanglement domain wall, with an additional weight q^2 given to trajectories that end at a position $y > x_0$ and a weight q given to trajectories ending at $y \leq x_0$, where x_0 is the location of the entangled reference qudit. The opposite weighting scheme is true for $\langle \text{Tr}\rho_A(t)^2 \rangle$. These additional weights arise due to the fact that, depending on the final position of the entanglement domain wall, the boundary spin at x is contracted with state $|\uparrow\rangle$ or $|\downarrow\rangle$. These overlaps are given in Eq. (4). With these expressions, it is straightforward to see that

$$I_{A,R}^{(\text{ann})}(t) = \log_q \left[\frac{q^2 - q(q-1)P(x_0, t)}{1 + (q-1)P(x_0, t)} \right], \quad (13)$$

where

$$P(x_0, t) \equiv \frac{1}{Z(t)} \sum_{y \geq x_0} z(y, t) \quad (14)$$

is the probability that the domain wall ends at a position $y \geq x_0$ at time t .

III. QUANTUM CODING TRANSITION

In this section, we study the behavior of the encoding of quantum information in the system, after evolving the system by the quantum circuit for T time steps, for a fixed dissipation strength p . The number of time steps of evolution T can be large so that $T/L \sim O(1)$, but is taken to be small enough throughout the entirety of this section, so that the left and right ends of the one-dimensional qudit chain are causally disconnected. As p is increased from zero, we find a ‘‘quantum coding’’ transition, where information initially encoded in the system is lost to the environment above a threshold $p = p_c$.

A. Annealed mutual information, and the pinning of an Ising domain wall

First, we investigate the behavior of $I_{A,R}^{(\text{ann})}$ as the dissipation strength p is tuned, by studying the Ising lattice magnet that emerges after performing a Haar average over the unitary gates in the quantum circuit acting on a qudit chain.

As discussed in Sec. II B, the partition sum $Z(T)$ describes a single Ising domain wall that can propagate through the bulk of the two-dimensional system, and be created or annihilated at the left boundary of the system. Tuning the dissipation strength, which alters the Ising symmetry-breaking field applied at the boundary, modulates an effective ‘‘pinning potential’’ for the Ising domain wall. This can be clearly seen in the limiting cases when $p = 0$ and $p = 1$. In the former case, the dissipation is completely absent, and Eq. (5) implies that the all-down state is left invariant by the transfer matrix for the Haar-averaged circuit. Thus, in this limit, there is no Ising domain wall. In contrast, when $p = 1$, the boundary spin is fixed in the $|\uparrow\rangle$ state, and the domain wall is effectively repelled from the left boundary.

Increasing the dissipation strength can then drive a pinning-depinning phase transition for the entanglement domain wall. Similar phase transitions due to the presence of a boundary magnetic field in an Ising magnet have been studied in the literature (see, e.g., Refs. [55–57]). Equivalently, the temporally directed nature of the Ising domain wall also suggests that these paths may be thought of as the imaginary-time trajectories of a single quantum mechanical particle on the half-line, which experiences a potential near the boundary, which is

tuned by the dissipation strength. Thus, $Z(T)$ is an amplitude for this particle to propagate under imaginary-time evolution by this Hamiltonian. In this setting, the particle can undergo a localization transition when the potential is *sufficiently* attractive [56]. This result is to be contrasted with the well-studied problem of a particle on the full line, with a delta-function potential near the origin, which always forms a bound state in the potential well as long as the potential is attractive.

The annealed mutual information precisely measures the localization of the Ising domain wall, as is evident from Eq. (13). Deep within a localized phase, where the transverse wandering of the domain wall is governed by a length scale ℓ_\perp , the probability $P(x_0, T) \sim e^{-x_0/\ell_\perp}$ ($\ell_\perp \ll x_0$), so that $I_{A,R}^{(\text{ann})}$ is a constant, deviating from its maximal value of 2 by a constant correction that changes within the localized phase. In contrast, in the delocalized phase, the probability $P(x_0, T) \stackrel{T \rightarrow \infty}{=} 1$, where the limit is taken, keeping the ratio $T/L = \text{const.}$ fixed.

Properties of this coding transition, as seen by annealed-averaged observables, such as the annealed mutual information, may be obtained by studying the lattice partition function for the Ising domain wall, which we present in Appendix A, due to the technical nature of the calculations involved. From this study, we find the following.

- (1) The phase transition occurs at a probability p_c that varies as a function of the on-site Hilbert space dimension q . The behavior of p_c as q is tuned may be determined by studying the lattice partition function. In the limit $q \rightarrow \infty$, the coding transition is absent. Specifically, we find that

$$p_c = 1 - O(q^{-2}), \quad (15)$$

so that information is always preserved in the system in the limit that the on-site Hilbert space dimension is strictly infinite.

- (2) Near the phase transition, the annealed mutual information takes the universal scaling form

$$I_{A,R}^{(\text{ann})}(T) = T^{-\beta/\nu} F[T^{1/\nu}(p - p_c)], \quad (16)$$

where $\beta = 1/2$ and $\nu = 2$. The function $F(x) \sim x^\beta$ as $x \rightarrow -\infty$, and we used the standard notation with exponent β characterizing the scaling of the order parameter and ν governing the divergence of the correlation length in the temporal direction. This relation is obtained by determining that in the thermodynamic limit the annealed mutual information should vanish on approaching the transition as $I_{A,R}^{(\text{ann})} \sim \ell_\perp^{-1}$, where ℓ_\perp is the distance of a transverse excursion of the Ising domain wall in the pinned phase. Therefore, this length scale diverges

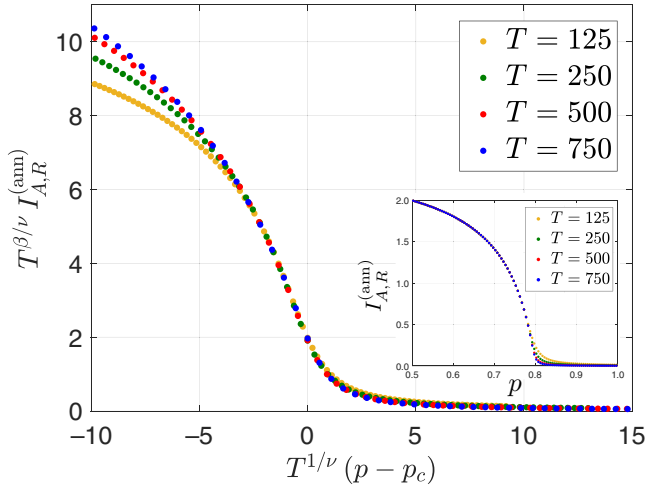


FIG. 3. Scaling collapse of the annealed mutual information, consistent with the scaling form in Eq. (16). The inset shows the behavior of the annealed mutual information as a function of dissipation strength p , indicating the presence of a coding transition. The exponents $\beta = 1/2$, $\nu = 2$ are determined from properties of the pinning transition of the Ising domain wall. The system size is taken to be large enough that the left and right ends of the qudit chain are causally disconnected.

as $\ell_{\perp} \stackrel{p \rightarrow p_c^-}{\sim} (p_c - p)^{-\beta}$ upon approaching the phase transition [58].

The above scaling form for the annealed mutual information is in good quantitative agreement with numerical studies, which we perform by directly studying the transfer matrix for the Ising magnet. A numerically obtained scaling collapse for the annealed mutual information is shown in Fig. 3, which is consistent with Eq. (16).

We expect that the qualitative behaviors presented here hold for the “quenched-averaged” quantities of interest, such as the averaged von Neumann mutual information $\langle I_{A,R}(t) \rangle$, which truly diagnose the loss of quantum information from the system, as the dynamics proceed. The true nature of the phase transition, however, will be different, as we discuss in Sec. III C below.

B. Numerical study

Having obtained a qualitative understanding of the coding transition by considering the “annealed” Haar average of the Rényi mutual information in general qudit systems, we now demonstrate the presence of this transition in numerical studies of quantum circuit evolution in a qubit chain ($q = 2$ on-site Hilbert space dimension). Here, the unitary time evolution of the bulk is governed by Clifford random unitary gates, arranged in a brickwork structure. This setup allows us to simulate the dynamics of large systems for sufficiently long times to study the phase transition introduced above, by relying on the

stabilizer formalism. We note that in a strict sense, Clifford random circuits do not display truly quantum chaotic behavior, intimately related to the fact that they can be efficiently simulated on classical computers. Nevertheless, they capture several crucial characteristics of chaotic quantum many-body systems, in particular, linear entanglement growth and efficient operator spreading [12–14]. These properties ensure that Clifford circuits realize dynamical phases analogous to Haar-random circuits, and establish them as powerful tools for studying generic chaotic quantum systems [39]. In the setup we consider, the boundary dissipation is realized as a random erasure channel, acting on the leftmost qubit with probability p in each time step, by deleting the information stored in the qubit. In the stabilizer formalism, this boundary erasure channel is implemented by deleting all stabilizers acting nontrivially (as a nonidentity operator) on the leftmost qubit.

We note that besides the protocol described above, we also considered other forms of boundary dissipation and Clifford scrambling, all giving rise to similar results for the behavior of the mutual information. Specifically, we implemented an alternative dissipation channel, by applying a controlled-NOT (CNOT) gate entangling the boundary qubit with an environmental ancilla qubit that was subsequently traced out from the density matrix. Moreover, we considered protocols with sparse bulk scrambling, where each unitary gate in the brickwork structure is a random Clifford unitary with probability $p_U < 1$, but the trivial identity operator with probability $1 - p_U$. This setup allowed us to tune the efficiency of the scrambling through parameter p_U , while keeping the boundary noise fixed, leading to a phase transition similar to that discussed in the main text. We discuss these alternative protocols in more detail, and present supplementary numerical results in Appendix B.

We encode a Bell pair in the initial state at the leftmost site, by entangling the boundary qubit with a reference qubit. In the notation introduced in Sec. II, this corresponds to the choice $x_0 = 0$. We note that the precise location of the encoding x_0 does not affect our results for the properties of the quantum coding transition, as long as x_0 takes a fixed finite value not scaling with the system size L . The remaining qubits are initialized in a random product state. We run the dissipative dynamics for time T , with the system size L chosen to keep $T/L < 1$ fixed, such that the right boundary of the system is not causally connected to the Bell pair. This setting allows us to detect the coding transition induced by a single boundary, by increasing the evolution time T . As noted in the introduction, performing the long time limit $T \rightarrow \infty$ and the thermodynamic limit $L \rightarrow \infty$ simultaneously allows us to probe the mutual information on timescales where the system is expected to become thermalized.

The mutual information $I_{A,R}$ between the output of the dissipative quantum circuit A and the reference qubit R is shown in Fig. 4 for different dissipation strengths p

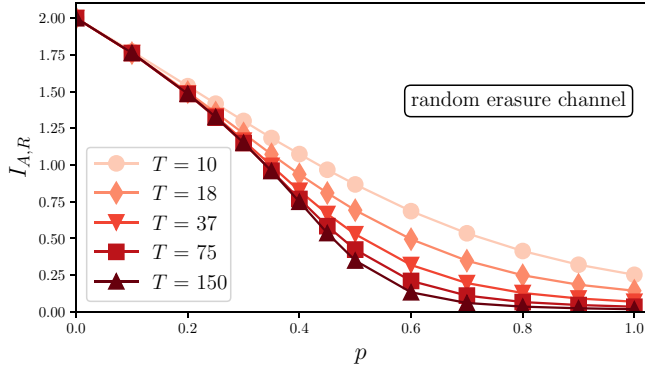


FIG. 4. Coding transition induced by a single boundary. The mutual information between the reference qubit and the output of the circuit shown as a function of dissipation strength p , for $T/L < 1$ fixed, with boundary dissipation realized as a random erasure channel. The scaling with circuit depths T points to a phase transition between a phase with partially protected information and a phase with all information lost.

and circuit depths T . These results are consistent with a coding transition tuned by the dissipation strength p , between a phase where the system retains part of the encoded information and a strongly dissipative phase with all information lost. We note that determining the critical exponents and critical point of this transition from finite time data is numerically challenging. Nevertheless, we attempt to estimate these parameters by noting that the mutual information obeys the finite-size scaling $I_{A,R} \sim T^{-\beta/\nu}$ at the critical dissipation strength p_c , while it saturates to a finite value as $T \rightarrow \infty$ for $p < p_c$. Relying on this observation, we identify p_c with the smallest p where the numerical data are consistent with $I_{A,R}$ approaching zero algebraically as $T \rightarrow \infty$, yielding the estimate $p_c \approx 0.5$. We then use the critical scaling $I_{A,R}|_{p=p_c} \sim T^{-\beta/\nu}$ to fit the ratio β/ν ; see Fig. 5(a). Finally, we estimate ν by requiring a good scaling collapse for the full set of data from Fig. 4. We obtain the critical parameters $p_c = 0.5$, $\beta/\nu = 0.34$, and $\nu = 2$, yielding the scaling collapse shown in Fig. 5(b). We note, however, that due to the large number of fitting parameters, the critical exponents extracted this way carry a considerable uncertainty. We leave the more thorough investigation of critical properties for future work.

C. The replica limit and the nature of the phase transition

The behavior of quenched-averaged quantities, e.g., the Haar-averaged Rényi mutual information $\langle I_{A,R}^{(2)}(t) \rangle$, close to the coding phase transition are quantitatively distinct from the annealed-averaged mutual information studied in Sec. III A. This observation is supported by the numerical studies of the previous section, which present strong evidence that the coding phase transition is in a different universality class from a depinning phase transition for

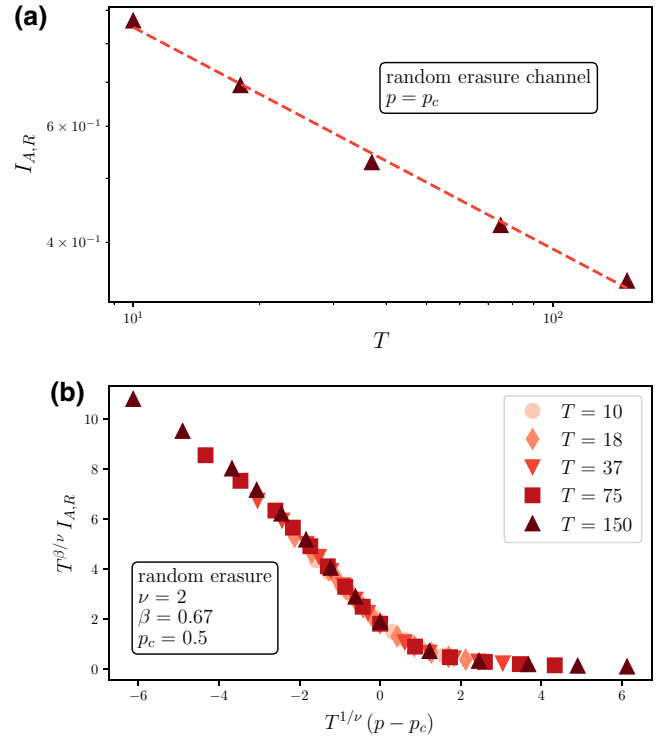


FIG. 5. Critical properties of the coding transition for a single boundary. (a) Critical power-law scaling of the mutual information with respect to circuit depth T at the estimated transition point, $p_c = 0.5$. The scaling relation $I_{A,R} \sim T^{-\beta/\nu}$ is used to extract $\beta/\nu = 0.34$ (dashed line). (b) Full scaling collapse of the rescaled mutual information $T^{\beta/\nu} I_{A,R}$ as a function of $T^{1/\nu} (p - p_c)$, using $\nu = 2$.

a single Ising domain wall. Here, we provide some conjectures on the nature of this phase transition, based on analytic arguments.

We focus our attention on the averaged second Rényi mutual information $\langle I_{A,R}^{(2)}(t) \rangle$ whose behavior may be obtained via a “replica trick”; the second Rényi entropy may be obtained in the limit $S_A^{(2)}(t) = \lim_{k \rightarrow 0} \{1 - [\text{Tr} \rho_A(t)^2]^k\}/k$, so that the calculation of the Haar-averaged mutual information reduces to evaluating quantities such as $\langle [\text{Tr} \rho_A(t)^2]^k \rangle$ in a replica limit $k \rightarrow 0$. After the Haar average, these quantities may be regarded as partition functions for lattice magnets with “spins” taking values in the permutation group on $2k$ elements S_{2k} [39]. A drastic simplification in the limit of large, but finite, on-site Hilbert space dimension q occurs [59], whereby $\langle [\text{Tr} \rho_A(t)^2]^k \rangle$ may be regarded as k copies of an Ising magnet, with weak inter-replica interactions at each spacetime point where a Haar-random unitary gate has been applied. The intrareplica interactions for each Ising magnet are described by the statistical mechanical rules presented in Sec. II A. The inter-replica interactions are known to be

attractive, and vanish in the limit that q is strictly infinite [59]. As already derived in Sec. II A, the boundary dissipation acts as an Ising symmetry-breaking field, giving rise to a boundary potential for the Ising domain wall within each replica.

The replica limit of the resulting theory may thus be regarded as the description of a directed path in a random environment [60,61], restricted to the half-line $x \geq 0$, and in the presence of a potential near this boundary, due to the dissipation. The path integral for this problem for a given realization of the disorder is formally given by

$$Z[V] = \int D_x(\tau) e^{-S[x, V]}, \quad (17)$$

where

$$S[x, V] \equiv \int d\tau \left[\frac{1}{2} \left(\frac{dx}{d\tau} \right)^2 + V[x, \tau] - u \delta[x] \right]. \quad (18)$$

Here $x(\tau)$ is the coordinate of the path at time τ . The random potential in the bulk $V[x, \tau]$ is taken to have zero mean, and is short-range correlated in spacetime, e.g., we may take the potential to be delta-function correlated as $\overline{V[x, \tau]V[x', \tau']} = \sigma^2 \delta(x - x') \delta(\tau - \tau')$, where $\overline{\cdot}$ denotes an average over the probability distribution for the disorder. The statistical mechanics of the replicated theory $\overline{Z^k}$ thus describes k interacting paths in the presence of a boundary potential, and thus resembles that of the Haar-averaged quantities $\langle [\text{Tr} \rho_A(t)^2]^k \rangle$, $\langle [\text{Tr} \rho_{A \cup R}(t)^2]^k \rangle$ in the limit of large, but finite, q . A schematic depiction of this replicated theory is shown in Fig. 6.

The weak inter-replica interactions are known to be a relevant perturbation at the critical point describing the pinning of a single Ising domain wall [62]. Remarkably, the new critical point describing the pinning or depinning of a directed polymer to an interface has been understood exactly [62] by Bethe ansatz techniques. The characteristic

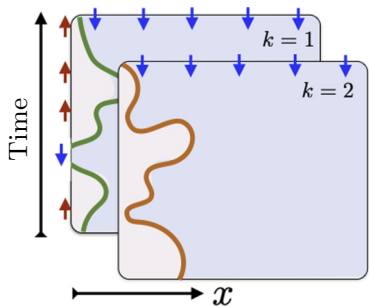


FIG. 6. The Haar-averaged Rényi mutual information between the reference qudit(s) and the system, $\langle I_{A,R}^{(2)}(t) \rangle$, is described in the large- q limit by k Ising domain walls in the presence of attractive, inter-replica interactions, and an attractive interface within each replica, in the limit $k \rightarrow 0$. This is described by the path integral in Eq. (18).

wandering length of the polymer transverse to the interface diverges with an exponent $\nu_{\perp} = 2$ on approaching the phase transition from the localized phase, while the divergence of the specific heat is characterized by the exponent $\alpha = 0$. For time-independent dissipation (e.g., the depolarizing channel is applied identically at the boundary at each time step of the quantum evolution), we thus expect the coding transition to be in the universality class of this depinning phase transition for a directed polymer.

In contrast, if the boundary dissipation varies randomly in time—as was studied in Sec. III B—then the nature of the phase transition is not completely understood. This problem corresponds to having an imaginary-time-dependent boundary potential $u(\tau) = u_0 + v(\tau)$ in Eq. (18), where $v(\tau)$ has zero mean and is short-range correlated in spacetime; for simplicity, we take $\overline{v(\tau_1)v(\tau_2)} = \mu^2 \delta(\tau_1 - \tau_2)$, with $\overline{\cdot}$ denoting the average over the distribution for $v(\tau)$.

We may study the relevance of randomness in this boundary potential at the depinning transition. Here, the action is invariant under coarse graining and rescaling $\tau' = \tau/b^z$ and $x' \equiv x/b$, where z is the dynamical critical exponent at the phase transition. Under this transformation, the random boundary potential becomes $\int d\tau v(\tau) \delta[x] \rightarrow b^{z-1} \int d\tau' v(b^z \tau') \delta[x']$, so that we identify $v'(\tau') \equiv b^{z-1} v(b^z \tau')$ as the renormalized potential in the coarse-grained theory. The correlations of the renormalized potential are thus

$$\overline{v'(\tau'_1)v'(\tau'_2)} = \mu^2 b^{z-2} \delta(\tau'_1 - \tau'_2). \quad (19)$$

Therefore, the strength of the disorder decreases under renormalization when $z < 2$. It has been conjectured [63] that $z = 3/2$ at the pinning transition for the directed polymer, so that the randomness in the boundary potential should be irrelevant by Eq. (19), so that the same fixed point describing the depinning of a directed polymer studied in Ref. [62] should describe the resulting transition in the presence of randomness.

We are, however, unaware of the correctness of this result in Ref. [63] for the dynamical exponent. The numerical studies presented in Sec. III B further suggest that $\nu_{\parallel} = 2$ (as opposed to $\nu_{\parallel} = z\nu_{\perp} = 3$, which is what would be predicted on the basis of $z = 3/2$ and $\nu_{\perp} = 2$), though more extensive numerical studies are required to pin down the nature of this transition [64]. We note, for completeness, that Eq. (19) suggests that the random boundary potential is a marginal perturbation exactly at the depinning phase transition for the Ising domain wall (which has $z = 2$ [57]). A Wilsonian renormalization-group calculation to higher order further suggests that the disorder is marginally *relevant* [65]. The nature of the resulting critical point is not understood, and deserves further investigation.

D. Perfect information protection using scrambling

In the low-dissipation phase of the coding transition, quantum information is only partially protected. One would expect that the information protection can be improved by first scrambling the information with unitary gates, which can effectively act like a random encoding, before the dissipation is turned on; we refer to this as a “prescrambling” step. Here we argue that, for fixed system size L and dissipation strength p , scrambling the initially local quantum information via a random unitary circuit of logarithmic depth $t_{\text{scr}} = k \log L$ for some sufficiently large k can lead to perfect protection of quantum information within the system, up to times of order $T \sim L/p$. For a prescrambling step with a fixed depth $t_{\text{scr}} = k \log L$ and for low k , we can observe the coding transition by tuning the dissipation strength p . The coding transition will now manifest in a step-function-like behavior of the mutual information $I_{A,R}$ across the transition, due to the perfect preservation of information for sufficiently low dissipation.

To gain some intuition for this result, we again consider the statistical mechanics of the Ising domain wall. As before, the domain wall is naturally thought of as propagating in a direction that is opposite to the arrow of time in the quantum circuit evolution. The domain wall thus propagates through T time steps of the circuit involving boundary dissipation, and then encounters the prescrambling step where the dissipation is absent. This corresponds to free evolution of the domain wall without the symmetry-breaking field at the boundary. When this field at the boundary is turned off, trajectories of the domain wall that have already been annihilated at the boundary—such as that shown in the left panel of Fig. 7—do not cost additional weights in the partition sum. On the other hand, “surviving” domain wall trajectories in the bulk—such as that shown in the right panel of Fig. 7—incur a weight

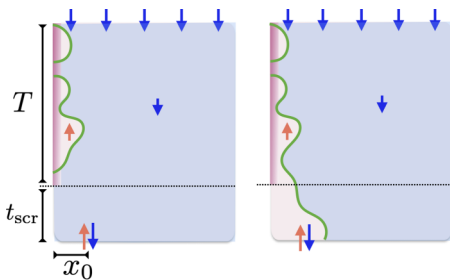


FIG. 7. The behavior of the Ising domain wall in the presence of a prescrambling step, whereby the initially local quantum information is evolved by a unitary quantum circuit of depth t_{scr} before the onset of dissipation. We consider propagation of the domain wall backwards in time, with respect to the arrow of time in the quantum circuit. In this picture, trajectories of the domain wall that survive in the bulk to the prescrambling step (right) are exponentially suppressed relative to trajectories that are annihilated at the boundary beforehand (left).

of $q/(q^2 + 1)$ at each time step. Thus, the weights of the bulk trajectories of the domain wall are exponentially suppressed in time relative to trajectories terminating at the boundary.

Let $Z_a(t, T)$ be the partition function for the Ising domain wall, after the T time steps of the dynamics with dissipation have taken place, followed by an additional t time steps of prescrambling, and so that the domain wall has been annihilated at the boundary of the system. In contrast, let $Z_b(t, T)$ be the partition function for the Ising domain wall to “survive” in the bulk of the system after the same evolution. To determine the behavior of the annealed mutual information, we wish to determine the probability that the domain wall ends at position $x \geq x_0$ after another t steps of the dissipation-free evolution, as per Eq. (13), where x_0 is the location of the entangled reference qubit of quantum information. For simplicity of presentation, we take x_0 to be at the boundary of the qubit chain, so that this probability $P(t, T)$ is

$$P(t, T) = \frac{Z_b(t, T)}{Z_a(t, T) + Z_b(t, T)}. \quad (20)$$

To make progress, we note that since the “surviving” trajectories contributing to $Z_b(t, T)$ are exponentially suppressed in time, we may write $Z_b(t, T) = Z_b(0, T)e^{-\gamma t}$, where γ is a phenomenological decay rate that will be a function of the local Hilbert space dimension and the dissipation strength. We further approximate the partition sum $Z_a(t, T)$ by its value before the prescrambling step, so that $Z_a(t, T) = Z_a(0, T)$. With these approximations, we may write

$$P(t, T) = \frac{P(0, T)}{P(0, T) + [1 - P(0, T)]e^{\gamma t}}. \quad (21)$$

The annealed mutual information is now obtained from Eq. (13). At sufficiently long times, so that $P(t, T) \ll 1$, we thus find that the mutual information deviates from its maximal value by

$$2 - I_{A,R}^{(\text{ann})}(t) = \frac{q^2 - 1}{q} \frac{P(0, T)}{P(0, T) + [1 - P(0, T)]e^{\gamma t}}. \quad (22)$$

In the pinned phase of the domain wall, we expect $P(0, T)$ to be exponentially small in the number of time steps T . In contrast, in the depinned phase, the probability that the domain wall has been annihilated at the interface decays as a power law in time due to the diffusive nature of the Ising domain wall, so that $P(0, T) = 1 - O(T^{-a})$, with a a constant. For fixed T , we thus find that, for a sufficiently long prescrambling time t , the mutual information deviates

from its maximal value as

$$2 - I_{A,R}^{(\text{ann})}(t) \sim \begin{cases} e^{-\gamma t}, & p < p_c, \\ T^a e^{-\gamma t}, & p > p_c. \end{cases} \quad (23)$$

Evaluating this expression at the scrambling time $t_{\text{scr}} = k \log L$ yields

$$2 - I_{A,R}^{(\text{ann})}(t) \sim \begin{cases} L^{-\gamma k}, & p < p_c, \\ L^{a-\gamma k}, & p > p_c. \end{cases} \quad (24)$$

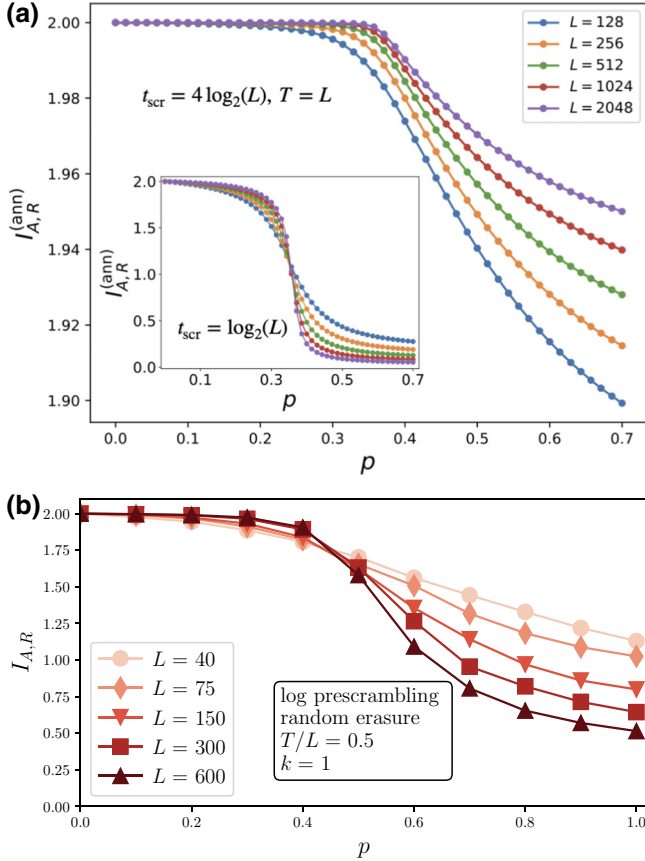


FIG. 8. Coding transition with logarithmic-depth prescrambling. In (a), $I_{A,R}^{(\text{ann})}$ versus p is plotted with a prescrambling circuit of depth $t_{\text{scr}} \sim \log L$. The subsequent evolution with dissipation proceeds for a total number of time steps $T = L$. The main plot is for $t_{\text{scr}} = 4 \log_2(L)$. The annealed mutual information approaches the maximum value as L is increased, indicating that logarithmic-depth encoding is enough to protect the information against boundary dissipation. Inset: plot for $t_{\text{scr}} = \log_2(L)$ with $I_{A,R}^{(\text{ann})}$ going through a transition with respect to p . The results agree with Eq. (24) derived in the text. In (b), we plot the mutual information calculated in Clifford dynamics as a function of dissipation strength p , applying prescrambling of depth $t_{\text{scr}} = \log_2(L)$. Boundary dissipation is realized as a random erasure channel, and $T/L = 1/2$ is kept fixed for different system sizes. The mutual information reveals a phase transition, with the critical point appearing as a crossing point of the data for different system sizes.

The above calculation implies that, for $t_{\text{scr}} = k \log L$, with large enough k , quantum information is perfectly preserved. Logarithmic scrambling is enough to protect the information against noise. For low values of k , the mutual information can exhibit different behavior depending on whether $a - \gamma k$ is positive or negative. We show the results obtained from studying the annealed mutual information numerically in Fig. 8(a), and find good agreement with the considerations above.

We now turn to the simulation of Clifford quantum circuit dynamics, restricting our attention to qubit chains. To explore how logarithmic prescrambling affects the coding transition induced by a single boundary, we modify the circuit protocol to include a unitary, nondissipative prescrambling step, with the prescrambling time scaling logarithmically with the system size, $t_{\text{scr}} = k \log L$, before applying the dissipative dynamics for time T . We then approach the thermodynamic limit by increasing T and L , while keeping the aspect ratio $T/L < 1$ fixed. In accordance with the insights gained above from the annealed Haar average, we find a phase transition for $k = 1$ as a function of p between a phase retaining information between the input and output of the circuit, and a phase with all information destroyed by dissipation, as shown in Fig. 8(b). The critical properties are different from the case without prescrambling discussed in the previous subsection, and, as predicted by the annealed model, the critical point is signaled by a crossing point in the mutual information obtained for different system sizes. We find a similar coding transition for $k \leq k_{\text{max}}$, with $k_{\text{max}} \sim O(1)$. For even larger values of k , the mutual information remains maximal for all values of p .

IV. CODING TRANSITION ON THE APPROACH TO THERMALIZATION

In the previous section, we studied systems of size L with dissipation acting near the left boundary in the regime $T \lesssim L$ so that the right boundary did not play a role in the dynamics. More precisely, as long as L/T remains larger than the velocity of the entanglement domain wall, which is less than the lightcone velocity in the quantum circuit, the coding transition can be understood as a depinning transition of the domain wall, such that, for noise rate p below the critical value p_c , some amount of information survives.

In this section, we study what happens when the dynamics in the coding phase extend for even longer periods of time, and show that the surviving information will eventually be lost to the environment as the system completely thermalizes. We may understand this result by considering the dynamics of the Ising domain wall, which describes the behavior of the annealed mutual information. For sufficiently large T/L , the domain wall will escape and get annihilated at the right boundary. Thus, using Eq. (13),

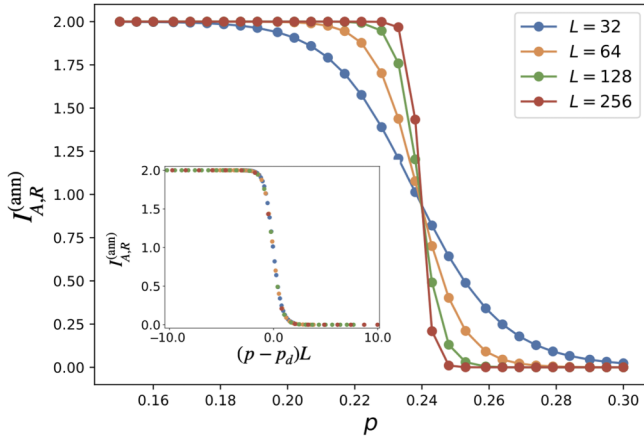


FIG. 9. Plot of $I_{A,R}^{(\text{ann})}$ in Haar-random circuits for $T/L = 4$ and $t_{\text{scr}} = L$. Inset: the data collapse to a single curve as a function of $(p - p_d)L$.

$I_{A,R}^{(\text{ann})}$ becomes zero and the information gets leaked to the environment. In this sense, the presence of the right boundary induces a phase transition at such large ratios T/L , which is qualitatively different from the transitions discussed in the previous sections. We can also interpret this phase transition in the original quantum circuit setup. In this language, the transition stems from the finite system size. Intuitively speaking, the system gets entangled with pT environment qudits, and when $pT \gtrsim L$, the system gets maximally entangled with the environment and becomes thermalized. By the monogamy of entanglement, the reference qudits can no longer be entangled with the system, but are lost to the environment [66]. Therefore, for large T/L , there is a transition with respect to the dissipation strength p , and the location of the critical point scales as $p_d \sim T/L$; for $p > p_d$, the information gets completely entangled with the environment. This transition is also visible with respect to T and for fixed dissipation strength p .

We study this coding transition by performing $t_{\text{scr}} = L$ steps of prescrambling before turning on the noise. As explained in the previous section, linear prescrambling perfectly protects the information for all strengths of dissipation, as long as T/L is sufficiently small. Because of this prescrambling step, the mutual information $I_{A,R}$ takes the shape of a “step function” as a function of dissipation strength, signaling the phase transition. We confirm this behavior by showing $I_{A,R}^{(\text{ann})}(T)$ versus p for $T/L = 4$ in a Haar-random circuit in Fig. 9. We also find a scaling collapse as a function of $(p - p_d)L$ (see the inset).

A. Numerical study

We also verify the above transition in the Clifford circuit setting acting on a qubit chain, introduced in the previous section. Here, after initializing a Bell pair at the left

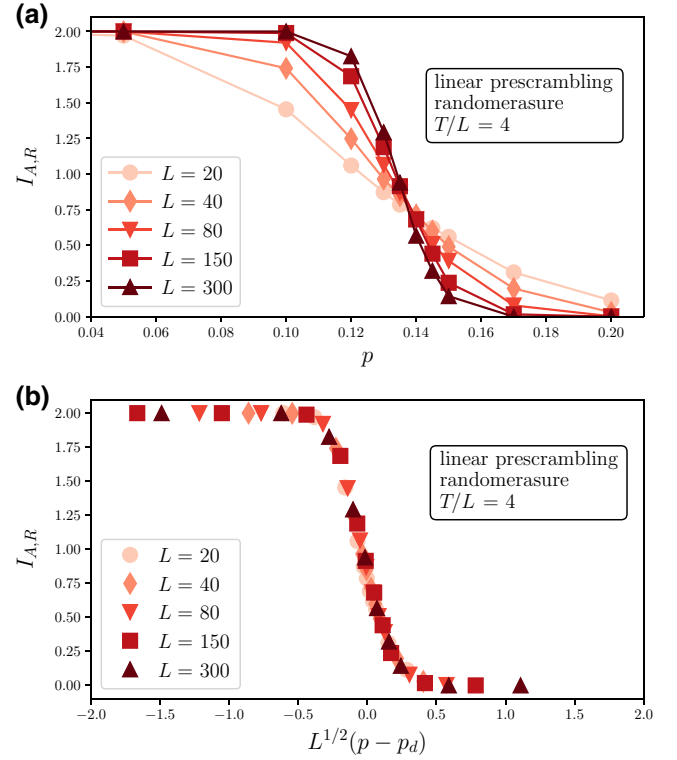


FIG. 10. Coding transition upon approaching thermalization. (a) Mutual information between the input and the output of the Clifford circuit shown as a function of dissipation strength p , converging towards a step function in the thermodynamic limit. Prescrambling time is set to $t_{\text{scr}} = L$, followed by dissipative dynamics for time T , with $T/L = 4$ fixed. (b) Data collapse as a function of $(p - p_d)L^{1/2}$, with the critical point $p_d = 0.136$ corresponding to the crossing point of finite-size data.

boundary of the chain, we run a prescrambling step linear in system size, $t_{\text{scr}} = L$, followed by the dissipative dynamics applied for time T . As before, we examine the finite-size scaling by increasing T and L , while keeping $T/L > 1$ fixed. As already discussed in the annealed framework, we find a phase transition for large enough aspect ratio $T/L > 1$. In Fig. 10(a), we plot the mutual information between the reference qubit and the output of the circuit as a function of p for different system sizes L , using a prescrambling time $t_{\text{scr}} = L$ and aspect ratio $T/L = 4$. In perfect agreement with the annealed picture, the mutual information curve approaches a step function in the thermodynamic limit, confirming a phase transition between a phase with all the information protected and a phase with all information destroyed.

We find a good scaling collapse with the scaling function depending on $(p - p_d)L^{1/2}$; see Fig. 10(b). The form of the scaling function differs from the annealed result. This deviation can be understood by noting that, for the annealed case, we applied a deterministic boundary depolarization

channel, Eq. (1), whereas the dissipation in the Clifford circuit is applied at random time steps, and this disorder may change the properties of the transition. Indeed, the effect of randomness in the dissipation channel can be studied by introducing disorder into the annealed model and applying channel (1) at random times, which leads to a scaling function depending on $(p - p_d)L^{1/2}$ (data not shown), in perfect agreement with the Clifford circuit results. The discrepancy between the factor of L and $L^{1/2}$ can be understood as follows. With randomness, the number of environment qubits entangled with the system increase linearly with T , but has fluctuations of order \sqrt{T} . This results in the critical point fluctuating as $\delta p/\sqrt{T}$, leading to $(p - p_d)L^{1/2}$ dependence of the mutual information.

B. Nature of the phase transition

We end this section by discussing the nature of the transition explored above. We argue below that the coding transition in this regime is a first-order phase transition.

To begin with, let us consider the large qudit limit such that $1/q \ll (1 - p)^2$. The partition function in the annealed picture contains contributions coming from all possible trajectories of the domain wall. The contribution at time t from trajectories having the domain wall at n_{DW} time steps is of order $(1/q)^{n_{\text{DW}}}[1 - p]^2 t^{-n_{\text{DW}}}$. The entropic factor, due to there being more configurations with the domain wall as opposed to without it, can only renormalize the $1/q$ factor. Thus, the partition function is dominated by the term having no domain wall at any point of time, $(1 - p)^{2t}$. However, for $(1 - p)^{2t} > (1/q)^L$, it is preferable for the domain wall to go all the way to the right boundary and get annihilated there. Thus, at $t_c \sim \log(1/q)L/\log(1 - p)$ the nature of the domain wall changes discontinuously from being stuck at the noisy boundary to getting annihilated at the un-noisy boundary, indicating a first-order transition. The finite q corrections to the above picture only act as thermal fluctuations, which causes the domain wall to have some excursions inside the bulk. The contributions from these excursions will be subleading and we expect the transition to remain first order. Note that similar timescales were also identified in Ref. [30] for the system to become perfectly thermalized in the presence of noise.

As in the standard theory of first-order phase transitions, the two boundaries correspond to the two local minima for the domain wall and the system discontinuously jumps from one to the other. The mutual information is then a function of the probability that the system is in one of the two minima [see Eq. (13)]. Since the free energy is extensive, the probability of being in a particular minimum scales as a function of δgV , where δg is the tuning parameter for the transition and V is the total volume of the system. In our case, the volume is equal to T . This explains the

observed finite-size collapse as a function of $(p - p_d)T$ in Fig. 9.

V. ENCODING AT A FINITE RATE

So far, we have focused on the dynamics of a single maximally entangled qudit pair localized near the noisy boundary. It is equally interesting to understand the effects of the noise when we have an extensive number of maximally entangled pairs in the initial state. We denote the code rate, defined as the fraction of the system's qudits entangled with reference qudits, by $C = N_R/L$, where N_R is the total number of maximally entangled pairs. For the purpose of this section, we consider code density $C = 1/2$, but we expect that the qualitative results should not change for different values of C as long as C is not close to 1. To

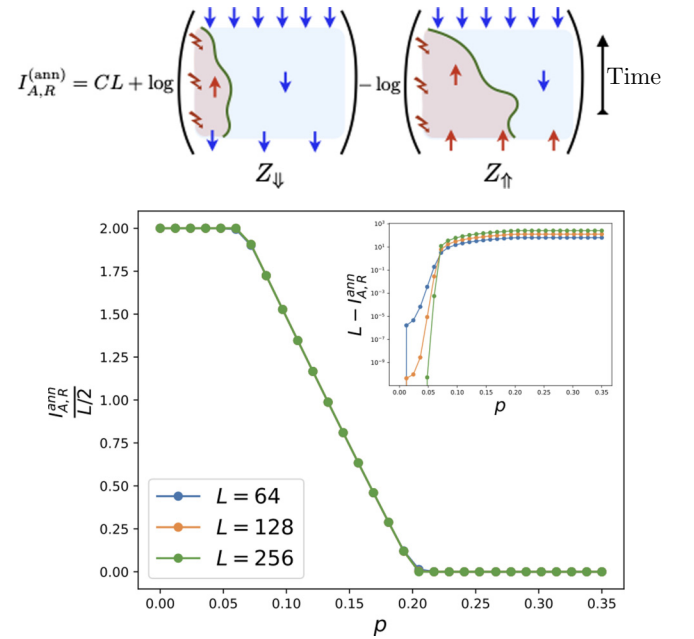


FIG. 11. Top: schematic representation of the statistical mechanics of the Ising domain wall in the calculation of the annealed mutual information, when coding at a finite rate. Typical domain wall trajectories when $p_{\text{th},1} < p < p_{\text{th},2}$ are shown. In Z_{\downarrow} the domain wall remains localized, whereas it is delocalized for Z_{\uparrow} , as explained in the text. Bottom: plot of the annealed mutual information in a qubit chain, measured between reference qubits entangled with the system's qubits at alternate sites ($C = 1/2$) and the system at the end of the dissipative evolution. The Bell pairs are prescrambled by a unitary circuit for time $t_{\text{scr}} = L$, after which the system is evolved in the presence of the boundary dissipation for time $T = 7L$. We find that, for $p < p_{\text{th}}^1 \approx 0.06$, full information is preserved, while for $p_{\text{th}}^1 < p < p_{\text{th}}^2 \approx 0.2$, a finite density of information is protected. The threshold values decrease as T is increased. Inset: for low $p < p_{\text{th}}^1$, there is no information loss even for $T = 7L$, that is, the difference between $I_{A,R}^{(\text{ann})}$ and the maximum value L goes to zero with the system size. Thus, all Bell pairs can be perfectly recovered by a recovery operation acting on the system.

make the final results independent of the spatial distribution of the maximally entangled pairs at the initial time, we apply random encoding by performing unitary scrambling for time $t_{\text{scr}} = L$.

We plot the annealed mutual information between the input and output, $I_{A,R}^{(\text{ann})}$, in Fig. 11 as a function of the dissipation strength for $T = 7L$. We find two threshold values for the noise rate, $p_{\text{th},1}, p_{\text{th},2}$. For $p < p_{\text{th},1}$, the information is perfectly protected and $I_{A,R}^{(\text{ann})}$ is equal to the maximal value $2CL$. For $p_{\text{th},1} < p < p_{\text{th},2}$, the information starts leaking to the environment, but a finite density of it still remains in the system. Finally, when $p > p_{\text{th},2}$, the information is completely leaked to the environment. Note that the values of p_{th} change with the ratio T/L .

Similarly to the strategy followed in the previous sections, we verify these predictions by performing numerical simulations on qubit chains subject to Clifford random quantum circuits. We show the density of the mutual information between the output of the circuit A and the reference qubits, $I_{A,R}/N_R$, with $N_R = L/2$ denoting the number of input Bell pairs, as a function of dissipation strength p in Fig. 12, for different system sizes L with $T/L = 4$ fixed. As noted above, here we applied a linear unitary prescrambling step for time $t_{\text{scr}} = L$, before the onset of the noisy dynamics, such that the results do not depend on the spatial distribution of the Bell pairs in the initial state. We find a phase with perfectly protected information for small enough dissipation strength p , followed by a crossover region with a finite density of preserved coherent information decreasing continuously with p , eventually decaying to zero for large p .

To understand this behavior, we again resort to the statistical mechanics of the Ising domain wall. The case of

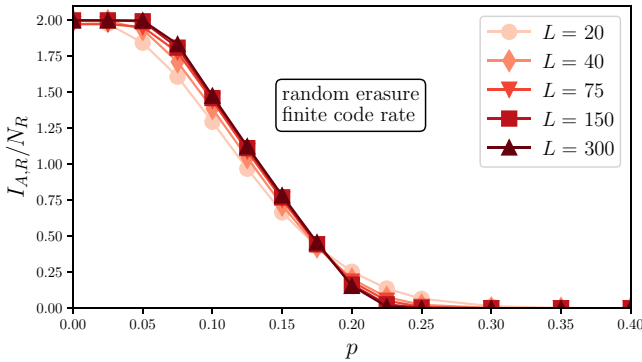


FIG. 12. Coding transition for a finite code rate. Density of the mutual information between the output of the circuit and the reference qubits shown as a function of dissipation strength p , for fixed evolution time $T/L = 4$ and $N_R = L/2$ initial Bell pairs. Prescrambling time is $t_{\text{scr}} = L$, followed by noisy dynamics with a random boundary erasure channel. The information density is perfectly protected for weak enough dissipation p , then decays continuously towards zero with p in a crossover region, with all information leaked to the environment for large enough p .

a finite code rate shows important differences compared to the model with an $O(1)$ amount of quantum information encoded. For a finite coding rate, there is an extensive number of Ising spins at the top boundary whose state is fixed by the boundary conditions, though the bulk dynamics of the domain wall remain the same. This leads to an exponential amplification of the trajectories that minimize the number of domain walls at the top boundary (note that these domain walls at the boundary are different from the Ising domain wall performing a random walk in the bulk). As shown at the top of Fig. 11, the annealed mutual information is given by

$$I_{A,R}^{(\text{ann})} = CL + \log_{\mathfrak{q}} \left(\frac{Z_{\downarrow}}{Z_{\uparrow}} \right), \quad (25)$$

where $Z_{\downarrow}, Z_{\uparrow}$, are the partition functions of the statistical mechanics model with down and up spins, respectively, at the locations of the encoded maximally entangled pairs. As discussed in Sec. IV, the domain wall discontinuously changes from being at the left boundary to being at the right boundary. To a good approximation, we can thus only keep these two trajectories in the partition function. For clarity of the expressions, we also introduce $\tilde{p} \equiv 1 - p$. The partition functions $Z_{\downarrow}, Z_{\uparrow}$ can thus be written as

$$Z_{\downarrow} \approx \tilde{p}^{2T} q^{2CL} + \left(\frac{1}{q} \right)^L q^{CL}, \quad (26)$$

$$Z_{\uparrow} \approx \tilde{p}^{2T} q^{CL} + \left(\frac{1}{q} \right)^L q^{2CL}. \quad (27)$$

Substituting the above expression into Eq. (25) and identifying the threshold values to be $1 - p_{\text{th},1} \sim q^{-(1-C)L/(2T)}$, $1 - p_{\text{th},2} \sim q^{-(1+C)L/(2T)}$, we get

$$I_{A,R}^{(\text{ann})} \approx \begin{cases} 2CL, & p < p_{\text{th},1}, \\ 2CL - 2T \log \left(\frac{1 - p_{\text{th},1}}{1 - p} \right), & p_{\text{th},1} < p < p_{\text{th},2}, \\ 0, & p > p_{\text{th},2}. \end{cases} \quad (28)$$

Intuitively, for low p , the domain wall remains localized near the noisy boundary and mutual information is maximal. As p is increased, it is easier for the domain wall in Z_{\uparrow} to delocalize compared to Z_{\downarrow} , as in the former, delocalization results in an exponential reduction in the cost associated with having domain walls at the boundary. Thus, the critical point at which the domain wall delocalizes is different for the two boundary conditions, resulting in the two thresholds discussed above.

VI. SUMMARY AND DISCUSSION

In this work, we studied one-dimensional quantum many-body systems with a noisy boundary. We focused on

the dynamics of the information of an initially localized maximally entangled qudit pair near the (noisy) boundary by studying the mutual information $I_{A,R}(t)$ between the inert reference qudit R of the pair and system A at late times. This is also related to the coherent information about the maximally entangled pair remaining in the system [52,53]. We find that the chaotic scrambling due to the unitary dynamics is sufficient to protect a part of this information against getting leaked to the environment for noise rate $p < p_c$ and long times $T \lesssim L/p$ by allowing the information to escape away from the boundary. We further show that a random encoding of the maximally entangled pair via noiseless scrambling dynamics of depth $\mathcal{O}(\log L)$ is sufficient to *perfectly* protect the information for all strengths of the noise up to time $T \lesssim L/p$. See Fig. 1(b) for a schematic representation of the phase diagram.

In the regime when the total time of evolution $T \gtrsim L/p$, any remaining information in the system is revealed to the environment and the system goes through a first-order coding transition. This transition can also be seen as a result of the system approaching thermalization to infinite temperature. We expect this form of coding transition to be present in all noisy channels, though in the case of the boundary noise considered here, the timescales associated with the transition increase parametrically with the system size [30].

We also consider the coding dynamics for a finite code rate, that is, when an extensive number, $N_R = CL$ with $C < 1$, of the system's qudits are entangled with reference qudits. We find that the code space can be *perfectly* preserved for noise strengths below some threshold $p_{\text{th},1}$, and for strengths above $p_{\text{th},2}$, the code space is completely destroyed; see Figs. 11 and 12. Equivalently, we can also extract the time for which the information stays in the system for a fixed noise rate p , and define two threshold times $T_{\text{th},1} < T_{\text{th},2}$, both of which scale linearly with the system size.

This work provides new insights into the competition between scrambling and decoherence. Normally, active feedback in the form of error correction is needed to counter the decoherence effects of the noise. However, we present the case of boundary noise where it is possible to have stable quantum error codes in the presence of generic noise, with the code space dynamically protected by scrambling. Previously, such dynamical protection of information was also observed for the special case of dephasing noise, which can be unraveled into quantum trajectories corresponding to projective measurements, but there an extensive number of ancilla qubits that act as a register for the measurement outcomes are made part of the system [27]. It would be of interest to generalize our results and techniques in the presence of ancilla qubits for cases different from the boundary noise. We leave this for future work.

Other interesting directions to explore are the presence of similar coding transitions in purely unitary evolution. It seems possible for quantum information to remain confined in part of a system evolving under chaotic unitary dynamics for a long time, and before the system thermalizes. We leave a detailed discussion of this direction to future work [67].

The competition between chaos and decoherence has also been studied in the context of open quantum systems. Previous studies have mostly focused on level statistics and quantities like the spectral form factor, purity, and the Loschmidt echo to study the effect of decoherence in chaotic dynamics [68–75]. It is an open question to study such probes in our context and whether the coding transitions can also be seen in these quantities. There is also a close relationship between the input-output mutual information and operator spreading [measured via out-of-time correlators (OTOCs)] in noise-free unitary dynamics [4]. It is interesting to understand how OTOCs in noisy systems are related to the emergent QEC property of the noisy dynamics [76–78]. Or, more generally, how is the dynamics of information related to the abovementioned quantities for open quantum systems?

The coding transitions imply protection of the code space against noise and the potential existence of a decoding protocol that brings back the code space to its initial state. Constructing such a protocol is notoriously hard for random dynamics having little structure, except in a few special cases like the Preskill-Hayden black hole protocol [1,79] or for special types of noise like the erasure channel. For Clifford circuits with boundary dissipation considered here, an efficient decoder can probably be constructed for the erasure channel and potentially also for depolarization noise [80]. Another interesting direction in further understanding the error-correcting properties of the coding transitions is to look into the code distance of the resulting code. We leave a detailed study of the decoding protocols and code distance for future studies.

We also find similar coding transitions for bulk defects where noise acts on the same site in the bulk. Protection of quantum information against bulk defects is important for the design of modular quantum computers, in which smaller modules of the quantum memory or computer are connected together to form a larger block. In this case, one expects the noise in the gates connecting the two modules to be far greater than the noise in the bulk of the individual modules. Thus, the existence of an error threshold against a bulk defect and the availability of the decoding protocol discussed above gives a fault-tolerant way of building a modular quantum computer.

A possible extension of our work is to study information dynamics in noisy symmetric systems. The behavior of information in symmetric systems with local charge density in the presence of measurements has been shown to be qualitatively different from the case without

symmetry [81–84]. It is also known that systems with local charge conservation can have charge transport and long-time operator entanglement growth even in the presence of strong dephasing noise [85,86]. This may potentially lead to a more robust encoding of the information when the code space is spread across different charge sectors as opposed to being confined to one sector. We leave the exploration of this effect for future studies.

ACKNOWLEDGMENTS

The authors thank the Kavli Institute for Theoretical Physics (KITP), where this research was initiated and partly performed. The KITP is supported, in part, by the National Science Foundation under Grant No. NSF PHY-1748958. S.V. thanks Matthew Fisher for helpful discussions. U.A. thanks Ali Lavasani for helpful discussions. I.L. acknowledges support from the Gordon and Betty Moore Foundation through Grant GBMF8690 to UCSB. This work was supported by the Simons Collaboration on Ultra-Quantum Matter, which is a grant from the Simons Foundation (651440, U.A.). S.V. acknowledges the support of the W. M. Keck Foundation (Grant No. 9303).

APPENDIX A: LATTICE PARTITION FUNCTION AND THE ANNEALED PHASE TRANSITION

The annihilation of the Ising domain wall at the boundary, and the free propagation of the domain wall through the bulk describe two distinct phases that may be accessed by tuning the dissipation strength, as described in detail in Sec. II. Here, we make this connection precise by studying the lattice partition function for the domain wall using the weights derived in Sec. II A. We consider the quantum circuit evolution shown schematically in Fig. 13(a), where each site (in blue) denotes the action of a two-site unitary gate on a qudit chain, while dissipation (in orange) acts periodically on the boundary qudit. Let $Z(T)$ denote the partition function for the domain wall propagating for a time T , defined so that at the initial and final times, the domain wall is absent (i.e., has been annihilated at the $x = 0$ interface). This partition sum may be calculated as follows. First, we define $Z_a(t)$ to be the partition function when there is no domain wall for a time interval t (it has been annihilated), while $Z_f(t)$ is the partition function when the domain wall is created at the $x = 0$ interface, wanders, and first returns back to the interface after a time t , after which it is then annihilated (the domain wall is free). With these definitions, we observe that $Z_0(T)$ is given by summing over all possible domain wall histories as

$$Z(T) = Z_a(T) + Z_f(T) + \sum_{t < T} Z_a(t) Z_f(T - t) + \dots, \quad (\text{A1})$$

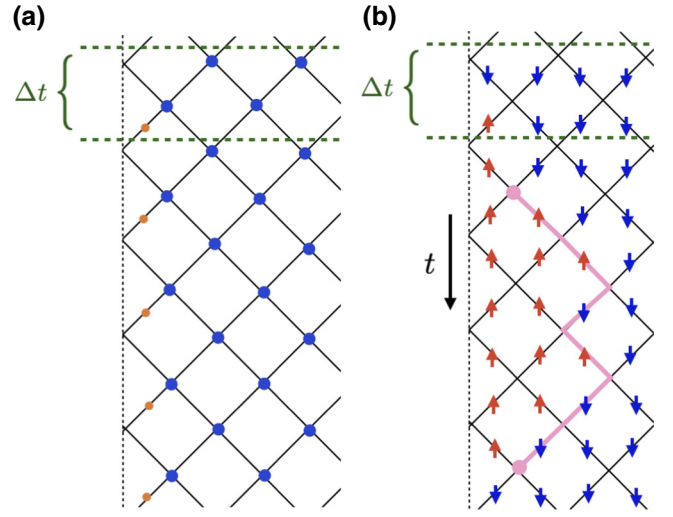


FIG. 13. A depiction of the quantum circuit that is applied to the qudit chain is shown in (a). Here, each blue vertex indicates the application of a two-site unitary gate, while the orange sites indicate the periodic application of a single-qudit depolarizing channel. The calculation of the corresponding Ising partition sum can be performed, with spin configurations living on bonds of the square lattice, as in (b), and which are naturally thought of as propagating in the indicated “time” direction by the transfer matrix for the Ising magnet. Shown is a contribution to $Z_f(t = 5)$, where the domain wall is created by the dissipation at the initial time, and is annihilated four time steps later. The trajectory of the Ising domain wall can be thought of as a path on the lattice, which starts from the first unitary gate that acts on a pair of antialigned spins, and ends when the domain wall is annihilated.

where the ellipsis denotes all possible domain wall configurations in which, at intermediate time steps, the domain wall wanders away or is annihilated at the interface.

It is convenient to consider the discrete Laplace transform of the partition function

$$z(w) \equiv \sum_{T \geq 0} w^T Z(T). \quad (\text{A2})$$

The inverse of this transformation is given by

$$Z(T) = \frac{1}{2\pi i} \oint_{\Gamma} dw \frac{z(w)}{w^{T+1}}, \quad (\text{A3})$$

where the contour Γ encloses the origin in the complex w plane. This relation is easily verified by substituting Eq. (A2). As a result, the smallest real singularity of $z(w)$ —denoted w_* —determines the behavior of the partition function at long times. Equivalently, the free-energy density $f = -T^{-1} \log Z$ is given by

$$f \stackrel{T \rightarrow \infty}{\sim} \log w_*. \quad (\text{A4})$$

The Laplace transform of $Z(T)$ is straightforward to evaluate, since each term in expansion (A1) is a discrete convolution of products of Z_a and Z_f . As a result, the Laplace transform of each term in this sum is simply the product of the Laplace transformations of appropriate products of Z_a and Z_f . We thus find that

$$z(w) = \frac{z_a(w) + z_f(w) + 2z_a(w)z_f(w)}{1 - z_a(w)z_f(w)} \quad (\text{A5})$$

with $z_a(w)$ and $z_f(w)$ defined as the Laplace transforms of $Z_a(t)$ and $Z_f(t)$, respectively.

Observe that $Z_a(t) = (1-p)^{2t}$ so that

$$z_a(w) = \frac{w(1-p)^2}{1 - w(1-p)^2}. \quad (\text{A6})$$

Similarly, we note that, when $t \geq 2$,

$$Z_f(t) = \frac{p(2-p)}{q} \left(\frac{q}{q^2+1} \right)^{2t-3} N_{2t-4}. \quad (\text{A7})$$

Here, $p(2-p)/q$ is the weight to create the Ising domain wall, as indicated in Eq. (7). The domain wall is acted upon by $2t-3$ two-site unitary gates, incurring a weight $q/(q^2+1)$ for the action of each gate. Finally, N_{2k} is the number of walks on the rotated square lattice—such as that shown in Fig. 13(b)—which start at a site closest to the boundary, and which return to the same point after $2k$ steps, without touching the boundary. This counting of paths is easily determined to be

$$N_{2k} = \binom{2k}{k} - \binom{2k}{k+1}. \quad (\text{A8})$$

Performing the Laplace transform thus yields

$$z_f(w) = \frac{p(2-p)}{2q} \frac{w(q^2+1)}{q} \left[1 - \sqrt{1 - \frac{w}{w_1(q)}} \right], \quad (\text{A9})$$

which has a singularity when the argument of the square root vanishes at

$$w_1(q) \equiv (q^2+1)^2/4q^2. \quad (\text{A10})$$

We note that $z(w)$ is also singular at $w = w_2$ such that $z_a(w_2)z_f(w_2) = 1$. Finally, we note that, while $z_a(w)$ contains a pole at $w = 1/(1-p)^2$, it is clear from Eq. (A5) that this does not give rise to a singularity in $z(w)$.

When $p > p_c$, the smallest real singularity of $z(w)$ occurs at $w = w_1(q)$, so that the free energy

$$f = 2 \log \left(\frac{q^2+1}{2q} \right), \quad p > p_c. \quad (\text{A11})$$

A phase transition occurs at $p = p_c$ when the two singularities merge, $w_1 = w_2$, and for $p < p_c$, the singularity

at $w_* = w_2$ determines the free-energy density. The phase transition therefore occurs when

$$z_f(w_1)z_a(w_1) = 1. \quad (\text{A12})$$

This equation may be solved numerically to obtain p_c for any finite q . The critical probability increases with increasing Hilbert space dimension q . In the limit $q \rightarrow \infty$, we may analytically solve this equation to find that p_c approaches one as

$$p_c = 1 - O(q^{-2}), \quad (\text{A13})$$

so that the phase transition is absent when the on-site Hilbert space dimension is strictly infinite.

Finally, we may study the singular part of the free energy near the transition at $p = p_c$. Expanding the equation $z_f(w_2)z_a(w_2) = 1$ for $p = p_c - \delta p$ with $\delta p \ll p_c$ yields the result that the singularity $w_* = w_2 = w_1 - \delta w$, where $\delta w \sim (\delta p)^2$. As a result, the free-energy difference vanishes when approaching the critical point as

$$\Delta f(p) \equiv f(p_c) - f(p) \stackrel{p \rightarrow p_c^-}{\sim} (p - p_c)^2. \quad (\text{A14})$$

On general grounds, the singular part of the free-energy density should vanish as $\Delta f \sim 1/\xi_{\parallel}$, where ξ_{\parallel} is the correlation length along the time direction. This correlation length thus diverges as $\xi_{\parallel} \sim (p - p_c)^{-\nu_{\parallel}}$ with $\nu_{\parallel} = 2$.

Finally, we may determine the typical length of an excursion ℓ_{\perp} that the domain wall will make into the bulk of the quantum circuit, and how this distance diverges as we approach the phase transition from the pinned phase $p \leq p_c$. First, observe that the weight for the Ising domain wall to make an excursion for a time t is $Z_f(t)/Z(t)$. Then the typical duration of an excursion is

$$\tau = \frac{\sum_t t Z_f(t)/Z(t)}{\sum_t Z_f(t)/Z(t)} \sim \frac{\sum_t t w_*^t Z_f(t)}{\sum_t w_*^t Z_f(t)} = \left. \frac{\partial \ln Z_f(w)}{\partial \ln w} \right|_{w=w_*},$$

where in the second expression, we have used the fact that $Z(t) \stackrel{t \rightarrow \infty}{\sim} w_*^{-t}$. On approaching the transition from the localized phase $p = p_c - \delta p$, the singularity $w_* = w_2 = w_1 - \delta w$ with $\delta w \sim \delta p^2$, as derived previously, which yields the result that $\tau \sim (p_c - p)^{-1}$ as $p \rightarrow p_c^-$. Assuming a diffusive wandering of the domain wall, the transverse distance covered by the domain wall diverges on approaching the depinned phase as

$$\ell_{\perp} \stackrel{p \rightarrow p_c^-}{\sim} (p_c - p)^{-1/2}. \quad (\text{A15})$$

Approaching the phase transition, when $\ell_{\perp} \gg x_0$, the probability that the domain wall has reached a point $y \geq x_0$ is approximately $P(x_0, t) = 1 - O(x_0/\ell_{\perp})$. Substituting this into Eq. (13) yields the result that the annealed

mutual information vanishes as $I_{A,R}^{(\text{ann})} \sim \ell_{\perp}^{-1} \sim (p_c - p)^{\beta}$ (with $\beta \equiv 1/2$) when approaching the phase transition. This behavior, along with the knowledge of $\nu_{\parallel} = 2$ motivates the finite-size scaling form for the annealed mutual information, which we use in the main text, $I_{A,R}^{(\text{ann})}(T) = T^{-\beta/\nu} F[T^{1/\nu}(p - p_c)]$.

APPENDIX B: ALTERNATIVE RANDOM CIRCUIT PROTOCOLS

To show that the phase transition in the mutual information persists irrespective of the precise form of the boundary dissipation and scrambling dynamics, here we introduce and examine four different protocols for the random circuit acting on a qubit chain. We consider the following two types of time evolution, each of them with two different realizations of the boundary dissipation.

(a) *Random boundary dissipation + maximal Clifford scrambling.* In each time step, the dissipation acts on the leftmost qubit with probability p . Scrambling is provided by random Clifford gates arranged in a brickwork structure. Therefore, the relative strength

of the dissipation compared to the efficiency of scrambling is tuned through parameter p .
 (b) *Periodic boundary dissipation + sparse Clifford scrambling.* The dissipation acts on the leftmost qubit periodically, with periodicity T_{period} . The unitary gates providing the scrambling of information are applied in a sparse brickwork structure, where each gate in the brickwork is a random Clifford unitary with probability p_U , and the identity with probability $1 - p_U$. In this setup, the relative strength of the dissipation compared to the efficiency of scrambling is determined by two parameters, T_{period} and p_U .

As described in the main text, the Bell pair is encoded in the initial state at the left boundary, optionally followed by a prescrambling step logarithmic or linear in the system size, depending on the type of phase transition that we consider. We note that the prescrambling is realized by a full or sparse brickwork of Clifford unitary gates, in the first and second types of dynamics, respectively.

As mentioned above, we consider two different realizations of the boundary dissipation.

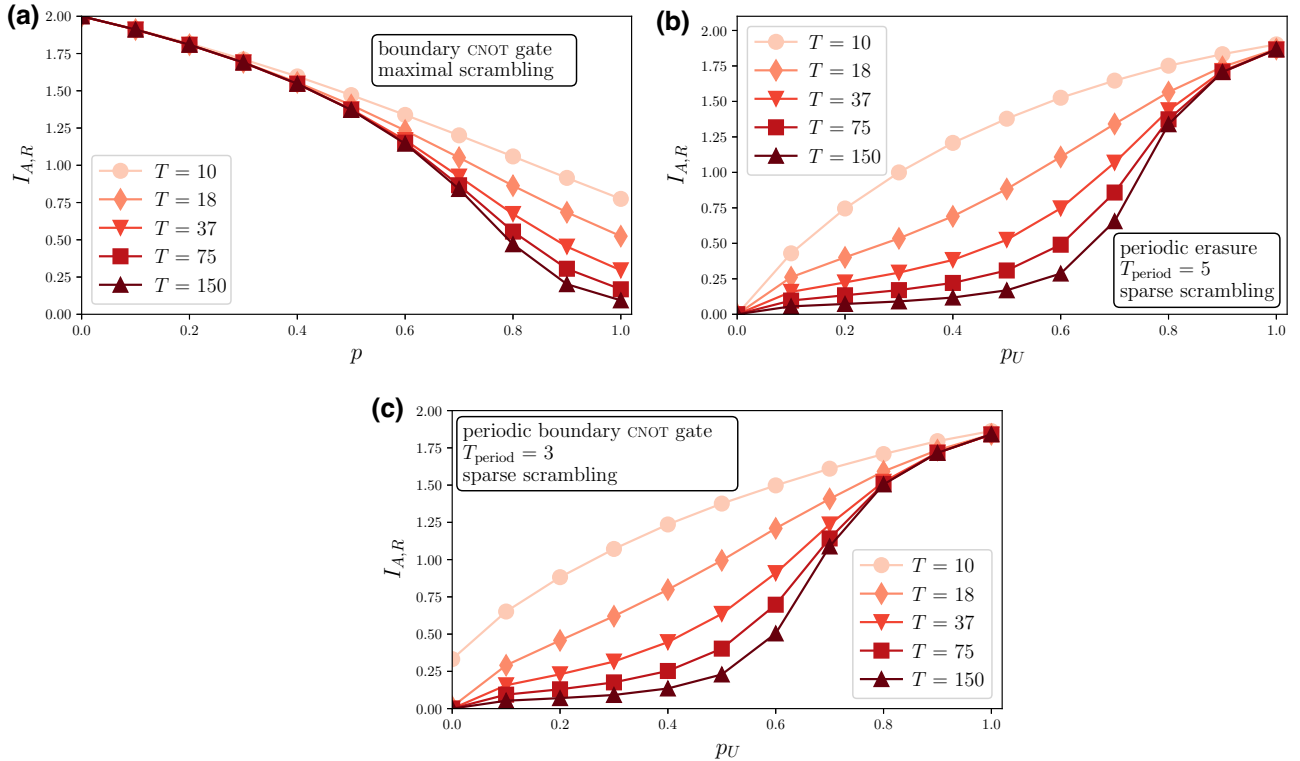


FIG. 14. Coding transition induced by a single boundary for different circuit protocols. Mutual information between the input and the output of the circuit (a) as a function of dissipation strength p for boundary dissipation realized as a CNOT coupling to an ancilla qubit with maximal bulk Clifford scrambling; (b),(c) varying the strength of sparse bulk Clifford scrambling p_U with a periodic boundary erasure channel (b) or a periodic boundary CNOT gate to an ancilla (c). All data are consistent with a coding transition between a phase with partially protected information for weak dissipation or strong enough scrambling, and a dissipative phase with all encoded information lost. No prescrambling step was used for these plots.

- (i) *Boundary erasure channel.* The dissipation acts by deleting the information stored in the leftmost qubit.
- (ii) *Coupling to an ancilla qubit.* Here, we first couple the leftmost qubit of the system to an ancilla qubit through a CNOT gate, and then trace out the ancilla. In the stabilizer formalism, this operation results in deleting all stabilizers containing a Y or Z Pauli operator at the left end of the chain. To restore rotational invariance and obtain a smooth limit $p_U \rightarrow 0$, for sparse Clifford scrambling, we also act with a random single-site Clifford gate on the leftmost qubit before applying the CNOT gate.

In the main text we mainly focused on the case of random boundary dissipation and maximal Clifford scrambling, with the dissipation realized as a boundary erasure channel. We also briefly commented on the effect of a periodic boundary noise, modifying the critical properties for linear prescrambling compared to the random case. Below we provide supplementary numerical results for the other protocols, showing a similar phase transition in the mutual information.

We show the coding transition in the mutual information without prescrambling, induced by a single boundary with aspect ratio $T/L < 1$, in Fig. 14 for three different protocols. We cross the phase transition by tuning the strength of dissipation p in Fig. 14(a), realized with a random CNOT coupling between the boundary spin and an ancilla qubit. In contrast, in Figs. 14(b) and 14(c) the tuning parameter is the strength of sparse bulk scrambling p_U , while we apply a fixed strength periodic boundary dissipation, realized as an erasure channel in Fig. 14(b) and as a CNOT gate with an ancilla qubit in Fig. 14(c). We recover the coding transition between a phase with partially protected coherent information and a phase where all information is destroyed for all protocols. Because of the difficulties in fitting critical exponents from finite-size data mentioned in the main text, we leave the detailed study of critical properties for future work. In the cases with periodic boundary dissipation we used $T_{\text{period}} = 5$ (b) and $T_{\text{period}} = 3$ (c).

[1] P. Hayden and J. Preskill, Black holes as mirrors: Quantum information in random subsystems, *J. High Energy Phys.* **9**, 120 (2007).

[2] Y. Sekino and L. Susskind, Fast scramblers, *J. High Energy Phys.* **10**, 065 (2008).

[3] N. Lashkari, D. Stanford, M. Hastings, T. Osborne, and P. Hayden, Towards the fast scrambling conjecture, *J. High Energy Phys.* **2013**, 22 (2013).

[4] P. Hosur, X. L. Qi, D. A. Roberts, and B. Yoshida, Chaos in quantum channels, *J. High Energy Phys.* **2016**, 1 (2016).

[5] L. Carr, *Understanding Quantum Phase Transitions* (CRC Press, Boca Raton, FL, 2010).

[6] H. P. Breuer and F. Petruccione, *The Theory of Open Quantum Systems* (Oxford University Press, Great Clarendon Street, 2002).

[7] M. Müller, S. Diehl, G. Pupillo, and P. Zoller, in *Advances in Atomic, Molecular, and Optical Physics*, edited by P. Berman, E. Arimondo, and C. Lin, *Advances In Atomic, Molecular, and Optical Physics* (Academic Press, San Diego, CA, 2012), Vol. 61, p. 1.

[8] I. Carusotto and C. Ciuti, Quantum fluids of light, *Rev. Mod. Phys.* **85**, 299 (2013).

[9] A. J. Daley, Quantum trajectories and open many-body quantum systems, *Adv. Phys.* **63**, 77 (2014).

[10] J. Maldacena, S. H. Shenker, and D. Stanford, A bound on chaos, *J. High Energy Phys.* **2016**, 106 (2016).

[11] T. Xu, T. Scaffidi, and X. Cao, Does scrambling equal chaos?, *Phys. Rev. Lett.* **124**, 140602 (2020).

[12] A. Nahum, J. Ruhman, S. Vijay, and J. Haah, Quantum entanglement growth under random unitary dynamics, *Phys. Rev. X* **7**, 031016 (2017).

[13] A. Nahum, S. Vijay, and J. Haah, Operator spreading in random unitary circuits, *Phys. Rev. X* **8**, 021014 (2018).

[14] C. W. von Keyserlingk, T. Rakovszky, F. Pollmann, and S. L. Sondhi, Operator hydrodynamics, OTOCs, and entanglement growth in systems without conservation laws, *Phys. Rev. X* **8**, 021013 (2018).

[15] M. Mezei and D. Stanford, On entanglement spreading in chaotic systems, *J. High Energy Phys.* **2017**, 65 (2017).

[16] D. J. Luitz and Y. Bar Lev, Information propagation in isolated quantum systems, *Phys. Rev. B* **96**, 020406 (2017).

[17] P. W. Shor, Scheme for reducing decoherence in quantum computer memory, *Phys. Rev. A* **52**, R2493 (1995).

[18] A. M. Steane, Error correcting codes in quantum theory, *Phys. Rev. Lett.* **77**, 793 (1996).

[19] C. H. Bennett, D. P. DiVincenzo, J. A. Smolin, and W. K. Wootters, Mixed-state entanglement and quantum error correction, *Phys. Rev. A* **54**, 3824 (1996).

[20] E. Knill and R. Laflamme, Theory of quantum error-correcting codes, *Phys. Rev. A* **55**, 900 (1997).

[21] E. Knill, R. Laflamme, and W. H. Zurek, Resilient quantum computation: Error models and thresholds, *Proc. R. Soc. London, Ser. A* **454**, 365 (1998).

[22] D. Aharonov and M. Ben-Or, Fault-tolerant quantum computation with constant error rate, [arXiv:quant-ph/9906129](https://arxiv.org/abs/quant-ph/9906129).

[23] P. Shor, in *Proceedings of 37th Conference on Foundations of Computer Science* (IEEE Computer Society Press, Los Alamitos, CA, 1996), p. 56.

[24] Y. Li, X. Chen, and M. P. A. Fisher, Quantum Zeno effect and the many-body entanglement transition, *Phys. Rev. B* **98**, 205136 (2018).

[25] B. Skinner, J. Ruhman, and A. Nahum, Measurement-induced phase transitions in the dynamics of entanglement, *Phys. Rev. X* **9**, 031009 (2019).

[26] A. Chan, R. M. Nandkishore, M. Pretko, and G. Smith, Unitary-projective entanglement dynamics, *Phys. Rev. B* **99**, 224307 (2019).

[27] M. J. Gullans and D. A. Huse, Dynamical purification phase transition induced by quantum measurements, *Phys. Rev. X* **10**, 041020 (2020).

[28] S. Choi, Y. Bao, X.-L. Qi, and E. Altman, Quantum error correction in scrambling dynamics and measurement-induced phase transition, *Phys. Rev. Lett.* **125**, 030505 (2020).

- [29] K. Noh, L. Jiang, and B. Fefferman, Efficient classical simulation of noisy random quantum circuits in one dimension, *Quantum* **4**, 318 (2020).
- [30] Z. Li, S. Sang, and T. H. Hsieh, Entanglement dynamics of noisy random circuits, *Phys. Rev. B* **107**, 014307 (2023).
- [31] C. E. Shannon, A mathematical theory of communication, *Bell Syst. Tech. J.* **27**, 379 (1948).
- [32] R. Gallager, Low-density parity-check codes, *IRE Trans. Inf. Theory* **8**, 21 (1962).
- [33] R. Gallager, The random coding bound is tight for the average code (corresp.), *IEEE Trans. Inf. Theory* **19**, 244 (1973).
- [34] D. J. C. MacKay and R. M. Neal, Near Shannon limit performance of low density parity check codes, *Electr. Lett.* **32**, 1645 (1996).
- [35] T. Richardson and R. Urbanke, Efficient encoding of low-density parity-check codes, *IEEE Trans. Inf. Theory* **47**, 638 (2001).
- [36] W. Brown and O. Fawzi, in *2013 IEEE International Symposium on Information Theory* (IEEE, 2013).
- [37] W. Brown and O. Fawzi, Decoupling with random quantum circuits, *Commun. Math. Phys.* **340**, 867 (2015).
- [38] M. J. Gullans, S. Krastanov, D. A. Huse, L. Jiang, and S. T. Flammia, Quantum coding with low-depth random circuits, *Phys. Rev. X* **11**, 031066 (2021).
- [39] M. P. A. Fisher, V. Khemani, A. Nahum, and S. Vijay, Random quantum circuits, *Ann. Rev. Condens. Matter Phys.* **14**, 335 (2022).
- [40] A. C. Potter and R. Vasseur, in *Entanglement in Spin Chains: From Theory to Quantum Technology Applications* (Springer, Cham, Switzerland, 2022), p. 211.
- [41] S.-K. Jian, C. Liu, X. Chen, B. Swingle, and P. Zhang, Quantum error as an emergent magnetic field, [arXiv:2106.09635](https://arxiv.org/abs/2106.09635).
- [42] Y. Li and M. P. A. Fisher, Decodable hybrid dynamics of open quantum systems with \mathbb{Z}_2 symmetry, *Phys. Rev. B* **108**, 214302 (2023).
- [43] L. Sá, P. Ribeiro, T. Can, and T. c. v. Prosen, Spectral transitions and universal steady states in random Kraus maps and circuits, *Phys. Rev. B* **102**, 134310 (2020).
- [44] Z. Weinstein, Y. Bao, and E. Altman, Measurement-induced power-law negativity in an open monitored quantum circuit, *Phys. Rev. Lett.* **129**, 080501 (2022).
- [45] S. Liu, M.-R. Li, S.-X. Zhang, S.-K. Jian, and H. Yao, Universal Kardar-Parisi-Zhang scaling in noisy hybrid quantum circuits, *Phys. Rev. B* **107**, L201113 (2023).
- [46] Z. Weinstein, S. P. Kelly, J. Marino, and E. Altman, Scrambling transition in a radiative random unitary circuit, *Phys. Rev. Lett.* **131**, 220404 (2023).
- [47] R. Fan, S. Vijay, A. Vishwanath, and Y.-Z. You, Self-organized error correction in random unitary circuits with measurement, *Phys. Rev. B* **103**, 174309 (2021).
- [48] Y. Li and M. P. A. Fisher, Statistical mechanics of quantum error correcting codes, *Phys. Rev. B* **103**, 104306 (2021).
- [49] Y. Bao, S. Choi, and E. Altman, Theory of the phase transition in random unitary circuits with measurements, *Phys. Rev. B* **101**, 104301 (2020).
- [50] Y. Li, S. Vijay, and M. P. A. Fisher, Entanglement domain walls in monitored quantum circuits and the directed polymer in a random environment, *PRX Quantum* **4**, 010331 (2023).
- [51] The qudit density matrix $\rho \equiv \sum_{i,j} \rho_{ij} |i\rangle \langle j|$ is a state $|\rho\rangle \equiv \sum_{i,j} \rho_{ij} |i,j\rangle$ in the doubled Hilbert space on which the operator $\hat{\Phi}$ acts as $\hat{\Phi}|\rho\rangle = (1-p)|\rho\rangle + (p/q)\sum_i |i,i\rangle$.
- [52] B. Schumacher and M. A. Nielsen, Quantum data processing and error correction, *Phys. Rev. A* **54**, 2629 (1996).
- [53] B. Schumacher and M. D. Westmoreland, Approximate quantum error correction, *Quantum Inf. Process.* **1**, 5 (2002).
- [54] V. Balasubramanian, A. Kar, C. Li, O. Parrikar, and H. Rajgadia, Quantum error correction from complexity in Brownian SYK, *J. High Energy Phys.* **2023**, 71 (2023).
- [55] D. Abraham, Solvable model with a roughening transition for a planar Ising ferromagnet, *Phys. Rev. Lett.* **44**, 1165 (1980).
- [56] D. Abraham, Binding of a domain wall in the planar Ising ferromagnet, *J. Phys. A: Math. Gen.* **14**, L369 (1981).
- [57] J. Chalker, The pinning of a domain wall by weakened bonds in two dimensions, *J. Phys. A: Math. Gen.* **14**, 2431 (1981).
- [58] These arguments, predicting a temporal correlation exponent $\nu = 2$ and that ℓ_{\perp} diverges with the order parameter exponent $\beta = 1/2$, suggest that ℓ_{\perp} differs from the correlation length in the spatial direction. Instead, we expect that a second emergent length scale with an exponent ν/z governs spatial correlations, where z is the dynamical critical exponent. If ℓ_{\perp} indeed governs the spatial correlation length then it would imply that $z = 4$, which is highly unlikely given that the model includes a diffusing domain wall.
- [59] T. Zhou and A. Nahum, Emergent statistical mechanics of entanglement in random unitary circuits, *Phys. Rev. B* **99**, 174205 (2019).
- [60] D. A. Huse and C. L. Henley, Pinning and roughening of domain walls in Ising systems due to random impurities, *Phys. Rev. Lett.* **54**, 2708 (1985).
- [61] M. Kardar and Y.-C. Zhang, Scaling of directed polymers in random media, *Phys. Rev. Lett.* **58**, 2087 (1987).
- [62] M. Kardar, Depinning by quenched randomness, *Phys. Rev. Lett.* **55**, 2235 (1985).
- [63] R. Lipowsky and M. E. Fisher, Wetting in random systems, *Phys. Rev. Lett.* **56**, 472 (1986).
- [64] The exponents ν_{\parallel} and ν_{\perp} govern the correlation lengths in the temporal and spatial directions, respectively. The temporal behavior of the mutual information that is the central object of this study is determined by the former. Therefore, exponent ν introduced in Sec. III A corresponds to ν_{\parallel} . A detailed study of ν_{\perp} requires spatially resolving the quantum information content along the chain, and is outside the scope of this work.
- [65] S. Vijay and M. P. A. Fisher, Unpublished (2022).
- [66] This qualitative argument invoking the monogamy of entanglement can be made precise in the case of qubits, by relying on the Coffmann-Kundu-Wootters inequalities [87,88]. This relation imposes constraints on a particular entanglement measure, the so-called concurrence, of qubits.
- [67] I. Lovas, U. Agrawal, and S. Vijay, Unpublished (2023).
- [68] K. Kawabata, A. Kulkarni, J. Li, T. Numasawa, and S. Ryu, Dynamical quantum phase transitions in SYK Lindbladians, *Phys. Rev. B* **108**, 075110 (2023).

- [69] B. Yan, L. Cincio, and W. H. Zurek, Information scrambling and Loschmidt echo, *Phys. Rev. Lett.* **124**, 160603 (2020).
- [70] Z. Xu, L. P. García-Pintos, A. Chenu, and A. del Campo, Extreme decoherence and quantum chaos, *Phys. Rev. Lett.* **122**, 014103 (2019).
- [71] T. Can, Random Lindblad dynamics, *J. Phys. A Math. Gen.* **52**, 485302 (2019).
- [72] R. A. Jalabert and H. M. Pastawski, Environment-independent decoherence rate in classically chaotic systems, *Phys. Rev. Lett.* **86**, 2490 (2001).
- [73] Z. P. Karkuszewski, C. Jarzynski, and W. H. Zurek, Quantum chaotic environments, the butterfly effect, and decoherence, *Phys. Rev. Lett.* **89**, 170405 (2002).
- [74] F. M. Cucchietti, D. A. R. Dalvit, J. P. Paz, and W. H. Zurek, Decoherence and the Loschmidt echo, *Phys. Rev. Lett.* **91**, 210403 (2003).
- [75] A. Peres, Stability of quantum motion in chaotic and regular systems, *Phys. Rev. A* **30**, 1610 (1984).
- [76] T. Schuster and N. Y. Yao, Operator growth in open quantum systems, [arXiv:2208.12272](https://arxiv.org/abs/2208.12272).
- [77] P. Zanardi and N. Anand, Information scrambling and chaos in open quantum systems, *Phys. Rev. A* **103**, 062214 (2021).
- [78] B. Yoshida and N. Y. Yao, Disentangling scrambling and decoherence via quantum teleportation, *Phys. Rev. X* **9**, 011006 (2019).
- [79] B. Yoshida and A. Kitaev, Efficient decoding for the Hayden-Preskill protocol, [arXiv:1710.03363](https://arxiv.org/abs/1710.03363).
- [80] A. S. Darmawan, Y. Nakata, S. Tamiya, and H. Yamasaki, Low-depth random Clifford circuits for quantum coding against Pauli noise using a tensor-network decoder, [arXiv:2212.05071](https://arxiv.org/abs/2212.05071).
- [81] U. Agrawal, A. Zabalo, K. Chen, J. H. Wilson, A. C. Potter, J. Pixley, S. Gopalakrishnan, and R. Vasseur, Entanglement and charge-sharpening transitions in U(1) symmetric monitored quantum circuits, *Phys. Rev. X* **12**, 041002 (2022).
- [82] F. Barratt, U. Agrawal, A. C. Potter, S. Gopalakrishnan, and R. Vasseur, Transitions in the learnability of global charges from local measurements, *Phys. Rev. Lett.* **129**, 200602 (2022).
- [83] F. Barratt, U. Agrawal, S. Gopalakrishnan, D. A. Huse, R. Vasseur, and A. C. Potter, Field theory of charge sharpening in symmetric monitored quantum circuits, *Phys. Rev. Lett.* **129**, 120604 (2022).
- [84] H. Oshima and Y. Fuji, Charge fluctuation and charge-resolved entanglement in a monitored quantum circuit with U(1) symmetry, *Phys. Rev. B* **107**, 014308 (2023).
- [85] D. Wellnitz, G. Preisser, V. Alba, J. Dubail, and J. Schachenmayer, Rise and fall, and slow rise again, of operator entanglement under dephasing, *Phys. Rev. Lett.* **129**, 170401 (2022).
- [86] Z. Cai and T. Barthel, Algebraic versus exponential decoherence in dissipative many-particle systems, *Phys. Rev. Lett.* **111**, 150403 (2013).
- [87] V. Coffman, J. Kundu, and W. K. Wootters, Distributed entanglement, *Phys. Rev. A* **61**, 052306 (2000).
- [88] T. J. Osborne and F. Verstraete, General monogamy inequality for bipartite qubit entanglement, *Phys. Rev. Lett.* **96**, 220503 (2006).